

# Mechanistic Studies of the Inactivation of Inducible Nitric Oxide Synthase by *N*<sup>5</sup>-(1-Iminoethyl)-L-ornithine (L-NIO)

Walter Fast,<sup>†,‡</sup> Dejan Nikolic,<sup>§</sup> Richard B. Van Breemen,<sup>§</sup> and Richard B. Silverman<sup>\*,†,||</sup>

Contribution from the Department of Chemistry and Department of Biochemistry, Molecular Biology, and Cell Biology, Northwestern University, Evanston, Illinois 60208-3113, and the Department of Medicinal Chemistry, University of Illinois at Chicago, Chicago, Illinois 60612-7231

Received July 2, 1998

**Abstract:** Nitric oxide synthase (NOS) catalyzes the conversion of L-arginine to L-citrulline and nitric oxide. *N*<sup>5</sup>-(1-Iminoethyl)-L-ornithine (L-NIO, **5**) is a natural product known to inactivate NOS, but the mechanism of inactivation is unknown. Upon incubation of iNOS with L-NIO a type I binding difference spectrum is observed, indicating that binding at the substrate binding site occurs. L-NIO is shown to be a time-dependent, concentration-dependent, and NADPH-dependent irreversible inhibitor of iNOS with  $K_I$  and  $k_{inact}$  values of  $13.7 \pm 1.6 \mu\text{M}$  and  $0.073 \pm 0.003 \text{ min}^{-1}$ , respectively. During inactivation the heme chromophore is partially lost (Figure 1); HPLC shows that the loss corresponds to about 50% of the heme. Inclusion of catalase during incubation does not prevent heme loss. *N*<sup>5</sup>-(1-Imino-2-[<sup>14</sup>C]ethyl)-L-ornithine (**11**) inactivates iNOS, but upon dialysis or gel filtration, no radioactivity remains bound to the protein or to a cofactor. The only radioactive product detected after enzyme inactivation is *N*<sup>ω</sup>-hydroxy-L-NIO (**12**); no *C*<sup>ω</sup>-hydroxy-L-NIO (**13**) or *N*<sup>δ</sup>-acetyl-L-ornithine (**14**) is observed (Figure 2). The amount of **12** produced during the inactivation process is  $7.7 \pm 0.2$  equiv per inactivation event. Incubations of **12** with iNOS show time-, concentration-, and NADPH-dependent inactivation that is not reversible upon dilution into the assay solution. Incubations that include an excess of L-arginine or with substitution of NADP<sup>+</sup> for NADPH result in no significant loss of enzyme activity. The  $K_I$  and  $k_{inact}$  values for **12** are  $830 \pm 160 \mu\text{M}$  and  $0.0073 \pm 0.0007 \text{ min}^{-1}$ , respectively. The magnitude of these kinetic constants (compared with those of **5**) suggest that **12** is *not* an intermediate of L-NIO inactivation of iNOS. Compound **12** also is a substrate for iNOS, exhibiting saturation kinetics with  $K_m$  and  $k_{cat}$  values of  $800 \pm 85 \mu\text{M}$  and  $2.22 \text{ min}^{-1}$ , respectively; the product is shown to be *N*<sup>δ</sup>-acetyl-L-ornithine (**14**) (Figure 3). The  $k_{cat}$  and  $k_{inact}$  values for **12** can be compared directly to give a partition ratio ( $k_{cat}/k_{inact}$ ) for inactivation of 304; i.e., there are 304 turnovers to give NO per inactivation event. This high partition ratio further supports the notion that **12** is *not* involved in L-NIO inactivation of iNOS. *C*<sup>ω</sup>-Hydroxy-L-NIO (**13**) is not an inactivator of iNOS. These results suggest that L-NIO inactivation occurs after an oxidation step (NADPH is required for inactivation) but prior to a hydroxylation step (**12** and **13** are not involved). Inactivation of iNOS by *N*<sup>5</sup>-(1-imino-2-[<sup>2</sup>H<sub>3</sub>]-ethyl)-L-ornithine (**15**) exhibits a kinetic isotope effect on  $^Hk_{inact}/^Dk_{inact}$  of  $1.35 \pm 0.08$  and on  $^H(k_{inact}/K_I)/^D(k_{inact}/K_I)$  of  $1.51 \pm 0.3$ , suggesting that the methyl C–H bond is cleaved in a partially rate-determining step prior to hydroxylation, and that leads to inactivation. A new NADPH-dependent 400 nm peak in the HPLC of L-NIO-inactivated iNOS is produced (Figure 4). LC–electrospray mass spectrometry (Figure 5) demonstrates the *m/z* of the new metabolite to be 583, which is shown to correspond to biliverdin (**23**) (Figures 6 and 7). Two possible mechanisms for the formation of biliverdin during inactivation are proposed (Schemes 10 and 11). When **14** is incubated with iNOS, time-, concentration-, and NADPH-dependent loss of enzyme activity is observed ( $K_I$  and  $k_{inact}$  values are 490 mM and  $0.24 \text{ min}^{-1}$ , respectively); iNOS inactivation by **14** can be prevented by inclusion of L-arginine, but not D-arginine, in the inactivation mixtures, suggesting that the inactivator acts at the arginine binding site. However, **14** is not produced from L-NIO (Figure 2) and, therefore, is *not* involved in L-NIO inactivation.

## Introduction

The relatively recent interest in nitric oxide (NO) has arisen from the surprising discovery that NO serves as a biological

messenger and is synthesized *in vivo* from oxygen and L-arginine by the enzyme nitric oxide synthase (NOS, EC 1.14.13.39).<sup>1</sup> The importance of understanding the chemistry and biochemistry of NO has been highlighted in fields as diverse as immunology and reproductive technology, and the implication of NO overproduction in septic shock, rheumatoid arthritis, strokes, and Parkinson's disease (among numerous other disease states) has fueled an increasing interest in the unique enzymology of NOS, how its catalysis occurs, and how it can be inhibited.<sup>1</sup>

\* Address correspondence to this author at Department of Chemistry, Northwestern University. Phone: (847) 491-5653. Fax: (847) 491-7713. E-mail: Agman@chem.nwu.edu.

<sup>†</sup> Department of Biochemistry, Molecular Biology, and Cell Biology, Northwestern University.

<sup>‡</sup> Present address: Department of Chemistry, The Pennsylvania State University, 152 Davey Laboratory, University Park, PA 16802.

<sup>§</sup> University of Illinois at Chicago.

<sup>||</sup> Department of Chemistry, Northwestern University.

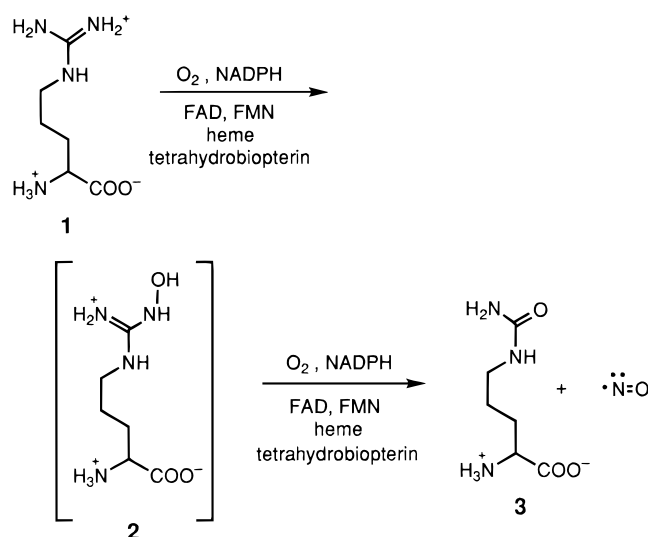
(1) Kerwin, J. F.; Heller, M. *Med. Res. Rev.* 1994, 14, 23–74.

NO has been implicated in numerous biological functions;<sup>2</sup> however, most systems can be grouped into one of three paradigms for NO function which correlate with three known isoforms of NOS: the immune response (inducible NOS or iNOS), smooth muscle relaxation (endothelial NOS or eNOS), and neuronal signaling (neuronal NOS or nNOS).

NOS has been shown to bind a number of cofactors including one FAD, one FMN, one NADPH, one protoporphyrin IX, and one tetrahydrobiopterin (BH<sub>4</sub>) per monomer. Each isoform is also calmodulin dependent, although iNOS has been shown to bind calmodulin tightly regardless of Ca<sup>2+</sup> concentration fluctuations.<sup>3</sup> NOS is active only as a disulfide-linked homodimer,<sup>4</sup> with each monomer consisting of two subdomains. Inspection of the NOS sequence and the crystal structure of iNOS<sup>5</sup> allows the identification of a C-terminal and N-terminal domain. The C-terminal domain of NOS shows a high sequence similarity to cytochrome P450 reductase and contains sequences for FAD, FMN, and NADPH binding sites.<sup>6</sup> This domain serves to shuttle electrons from the obligate two electron donor, NADPH, through the one or two electron acceptor/donors, FAD and FMN, to the N-terminal domain of the other monomer.<sup>7</sup> In the N-terminal domain, which binds the heme and tetrahydrobiopterin,<sup>8</sup> the tetrahydrobiopterin is suspected to be the initial electron acceptor, which subsequently transfers electrons to the heme where substrate oxidation occurs.<sup>9</sup> In the resting state, an air-stable flavin semiquinone (presumably FMNH<sup>•</sup>) has been detected by EPR.<sup>10</sup> Unlike the C-terminal domain, the N-terminal domain does not show any sequence similarity to known cytochrome P450 related proteins. In the resting state, NOS contains a ferric, five coordinate heme with a cysteine thiolate as the proximal axial ligand. The N-terminal and C-terminal domains are joined by a short sequence encoding a calmodulin binding site which serves as a sort of switch. Ca<sup>2+</sup>/calmodulin are required to allow electron transfer between the C-terminal and N-terminal domains.<sup>11</sup>

NOS converts L-arginine (**1**, Scheme 1) and O<sub>2</sub> to citrulline (**3**) and NO with the concomitant oxidation of NADPH. N<sup>ω</sup>-Hydroxy-L-arginine (**2**) has been shown to be a catalytically competent intermediate;<sup>12</sup> the hydroxyl group (and the ureido oxygen of citrulline) is derived from molecular oxygen (not bulk water).<sup>13</sup> Nitric oxide is derived from the guanidino nitrogen

### Scheme 1



of L-arginine<sup>14</sup> and from the corresponding nitrogen in N<sup>ω</sup>-hydroxy-L-arginine.<sup>12,15</sup> One NADPH is used in producing N<sup>ω</sup>-hydroxy-L-arginine (**2**), and 0.5 NADPH is used in conversion of this intermediate to citrulline and NO.

Because of its similarity to cytochrome P450s, various heme-based mechanisms have been proposed for the catalysis of L-arginine to NO and L-citrulline. Like cytochrome P450, carbon monoxide can inhibit both steps of the reaction (although at different levels<sup>16</sup>), implicating a role for the heme in each oxidation step.<sup>17</sup> Following precedence for N-hydroxylation of amidines by cytochrome P450s,<sup>18</sup> a classical P450 type mechanism involving a perferryl Fe–heme complex ([FeO]<sup>3+</sup>)<sup>19</sup> can be proposed for the first step in the reaction (Scheme 2). Formation of the perferryl Fe–heme complex usually requires a general acid derived from the enzyme.<sup>20</sup> No suitable residues are found in the hydrophobic distal heme pocket; however, substrate-assisted catalysis has been suggested.<sup>5,21</sup> As with the cytochrome P450 enzymes, uncoupled production of hydrogen peroxide<sup>22</sup> and superoxide<sup>23</sup> can be observed under certain conditions. Even though a similar perferryl Fe–heme type mechanism can be proposed for the second oxidation step, White and Marletta<sup>24</sup> suggest that, following hydrogen atom abstraction of **2**, the second oxidation may be more like that proposed for aromatase, also a multistep oxidative catalyst.<sup>25</sup> In the third step of aromatase, the electrophilicity of a substrate acyl-carbon

(2) Kerwin, J. F.; Lancaster, J. R.; Feldman, P. L. *J. Med. Chem.* **1995**, *38*, 4343–4362.

(3) Cho, H. J.; Xie, Q.; Calaycay, J.; Mumford, R. A.; Swiderek, K. M.; Lee, T. D.; Nathan, C. *J. Exp. Med.* **1992**, *176*, 599–604.

(4) Baek, K. J.; Thiel, B. A.; Lucas, S.; Stuehr, D. J. *J. Biol. Chem.* **1993**, *268*, 21120–21129.

(5) Crane, B. R.; Arvai, A. S.; Ghosh, D. K.; Wu, C.; Getzoff, E. D.; Stuehr, D. J.; Tainer, J. A. *Science* **1998**, *279*, 2121–2126.

(6) Bredt, D. S.; Hwang, P. M.; Glatt, C. E.; Lowenstein, C.; Reed, R. R.; Snyder, S. S. *Nature* **1991**, *351*, 714–718.

(7) Siddhanta, U. P., A.; Fan, B.; Wolan, D.; Rousseau, D. L.; Stuehr, D. J. *J. Biol. Chem.* **1998**, *273*, 18950–18958.

(8) Lambert, L. E.; French, J. F.; Whitten, J. P.; Baron, B. M.; McDonald, I. A. *Eur. J. Pharmacol.* **1992**, *216*, 131–134.

(9) Bec, N.; Gorren, A. C.; Voelker, C.; Mayer, B.; Lange, R. *J. Biol. Chem.* **1998**, *273*, 13502–13508.

(10) Stuehr, D. J.; Ikeda-Saito, M. *J. Biol. Chem.* **1992**, *267*, 20547–20550.

(11) (a) Abu-Soud, H. M.; Yoho, L. L.; Stuehr, D. J. *J. Biol. Chem.* **1994**, *269*, 32047–32050. (b) Sheta, E. A.; McMillan, K.; Siler-Masters, B. S. *J. Biol. Chem.* **1994**, *169*, 15147–15153.

(12) Stuehr, D. J.; Kwon, N. S.; Nathan, C. F.; Griffith, O. W.; Feldman, P. L.; Wiseman, J. *J. Biol. Chem.* **1991**, *266*, 6259–63.

(13) (a) Kwon, N. S.; Nathan, C. F.; Gilker, C.; Griffith, O. W.; Matthews, D. E.; Stuehr, D. J. *J. Biol. Chem.* **1990**, *265*, 13442–13445. (b) Leone, A. M.; Palmer, R. M. J.; Knowles, R. G.; Francis, P. L.; Ashton, D. S.; Moncada, S. *J. Biol. Chem.* **1991**, *266*, 23790–5.

(14) Tayeh, M. A.; Marletta, M. A. *J. Biol. Chem.* **1989**, *264*, 19654–8.

(15) Pufahl, R. A.; Nanjappan, P. G.; Woodard, R. W.; Marletta, M. A. *Biochemistry* **1992**, *31*, 6822–8.

(16) Campos, K. L.; Giovanelli, J.; Kaufman, S. *J. Biol. Chem.* **1995**, *270*, 1721–1728.

(17) Marletta, M. A. *J. Biol. Chem.* **1993**, *268*, 12231–12234.

(18) (a) Clement, B.; Jung, F.; Pfunder, H. *Mol. Pharmacol.* **1993**, *43*, 335–342. (b) Andronik-Lion, V.; Boucher, J. L.; Delaforege, M.; Henry, Y.; Mansuy, D. *Biochem. Biophys. Res. Commun.* **1992**, *185*, 452–458.

(19) Guengerich, F. P.; Macdonald, T. L. *Acc. Chem. Res.* **1984**, *17*, 9–16.

(20) Vaz, A. D. N.; Pernecky, S. J.; Raner, G. M.; Coon, M. J. *Proc. Natl. Acad. Sci. U.S.A.* **1996**, *93*, 4644–4648.

(21) Crane, B. R.; Arvai, A. S.; Gachhui, R.; Wu, C.; Ghosh, D. K.; Getzoff, E. D.; Stuehr, D. J.; Tainer, J. A. *Science* **1997**, *278*, 425–431.

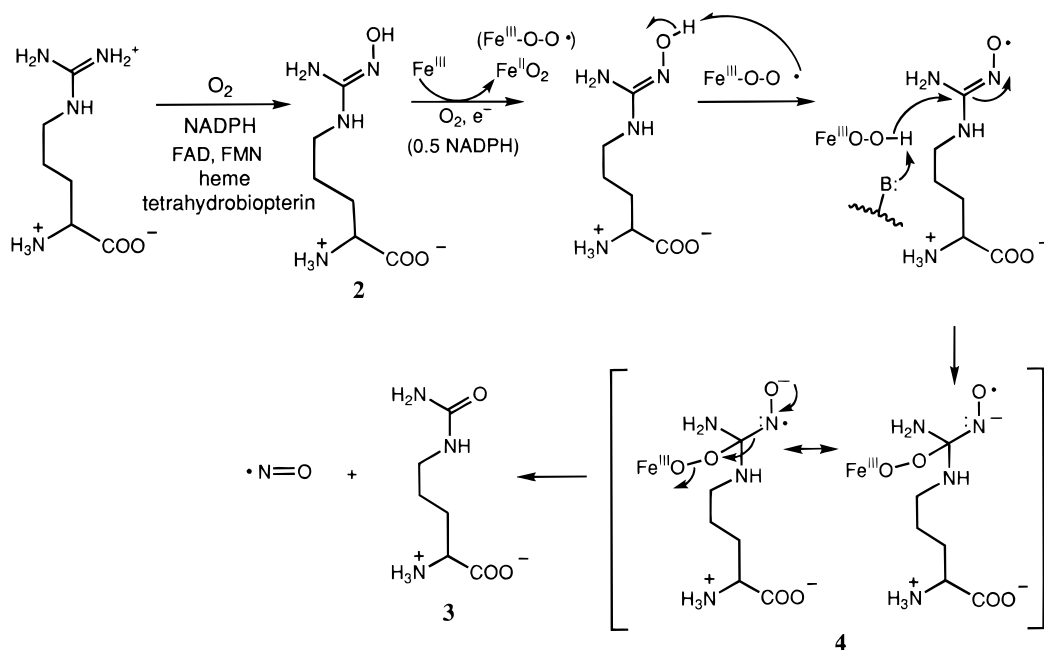
(22) Heinzel, B.; John, M.; Klatt, P.; Bohme, E.; Mayer, B. *Biochem. J.* **1992**, *281*, 627–630.

(23) Pou, S.; Pou, W. S.; Bredt, D. S.; Snyder, S. H.; Rosen, G. M. *J. Biol. Chem.* **1992**, *267*, 24173–24176.

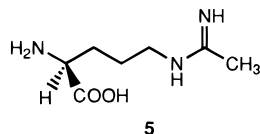
(24) White, K.; Marletta, M. A. *Biochemistry* **1992**, *31*, 6627–6631.

(25) (a) Akhtar, M.; Corina, D.; Miller, S.; Shyadehi, A. Z.; Wright, J. N. *Biochemistry* **1994**, *33*, 4410–4418. (b) Korth, H.; Sustmann, R.; Thater, C.; Butler, A. R.; Ingold, K. U. *J. Biol. Chem.* **1994**, *269*, 17776–17779.

Scheme 2



functionality is thought to trap a nucleophilic ferric peroxide (Fe<sup>III</sup>OOH) intermediate (4), which can then fragment to yield

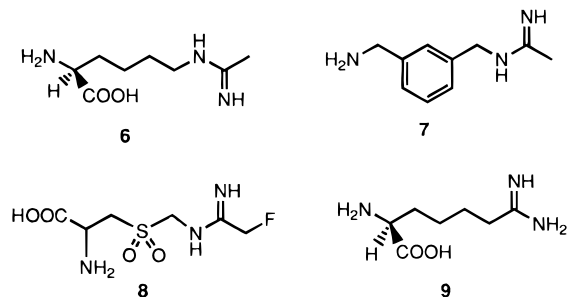


products. Chemical model studies for *N*<sup>ω</sup>-hydroxyguanidines also support the role of a nucleophilic hydroperoxy species in the catalytic mechanism for NOS.<sup>26</sup>

The arginine analogue *N*<sup>5</sup>-(1-iminoethyl)-L-ornithine (L-NIO) (5) was originally isolated as a natural product from an unclassified *Streptomyces*.<sup>27</sup> The structure and p*K*<sub>a</sub> values of L-NIO are very similar to those of L-arginine.<sup>27,28</sup> In fact, L-NIO can even serve as a substrate for the enzyme arginase, forming ornithine as a product, and it is served by the same cationic transport system (γ<sup>+</sup>).<sup>29</sup> Despite its structural similarities to L-arginine, L-NIO also inhibits some arginine-dependent enzymes; L-NIO inhibited a crude preparation of NOS.<sup>30</sup> Reversible inhibition of NOS by L-NIO has reported IC<sub>50</sub> values of 7.7, 5.8, and 10 μM for recombinant human inducible, endothelial, and neuronal NOS, respectively,<sup>31</sup> and, therefore, is not an isoform-selective inhibitor. The binding of L-NIO to the active site of nNOS, as characterized by EPR spectroscopy, shows spectral changes intermediate between those caused by

arginine-like and *N*<sup>ω</sup>-hydroxyarginine-like ligands, yet dissimilar to those caused by *N*<sup>ω</sup>-methylarginine-like or *N*<sup>ω</sup>-nitroarginine-like ligands.<sup>32</sup>

L-NIO is prototypical of a class of time-dependent carbamidine-containing NOS inhibitors. Other members of this class include *N*<sup>5</sup>-(1-iminoethyl)-L-lysine (L-NIL, 6; homo-L-NIO)<sup>33</sup>



and *N*-(3-(aminomethyl)benzyl)acetamidine (1400W, 7),<sup>34</sup> which contain the same pharmacophore and also demonstrate time-dependent inhibition as well as many of the characteristics of a mechanism-based inactivator. Probably the most thoroughly studied amidine-containing inactivator is 6. Inactivation of iNOS by 6 is time dependent, irreversible by dilution, and NADPH- and O<sub>2</sub>-dependent.<sup>35</sup> Reports of heme loss due to inactivation differ,<sup>35,36</sup> but inactivation seems to cause a destabilization of the iNOS homodimer into inactive monomers.<sup>36</sup> Use of radio-labeled 6 failed to indicate covalent protein modification or substrate oxidation.<sup>35,36</sup> Likewise, use of [<sup>14</sup>C-amidine]-labeled 7 did not show any turnover products, but the low specific activity of the compound prevented the detection of any E-I

(26) (a) Pufahl, R. A.; Wishnok, J. S.; Marletta, M. A. *Biochemistry* **1995**, *34*, 1930–1941. (b) Clague, M. J.; Wishnok, J. S.; Marletta, M. A. *Biochemistry* **1997**, *36*, 14465–14473. (c) Fukuto, J. M.; Stuehr, D. J.; Feldman, P. L.; Bova, M. P.; Wong, P. *J. Med. Chem.* **1993**, *36*, 2666–2670.

(27) Scannell, J. P.; Ax, H. A.; Pruess, D. L.; Williams, T.; Demny, T. C.; Stempel, A. *J. Antibiot.* **1972**, *25*, 179–184.

(28) Jencks, W. P.; Regenstein, J. Ionization Constants of Acids and Bases. In *Handbook of Biochemistry*; Sober, H. A., Ed.; Chemical Rubber Co.: Cleveland, OH, 1968; pp J-148–J189.

(29) Baydoun, A. R.; Mann, G. E. *Biochem. Biophys. Res. Commun.* **1994**, *200*, 726–731.

(30) McCall, T. B.; Feelisch, M.; Palmer, R. M. J.; Moncada, S. *Br. J. Pharmacol.* **1991**, *102*, 234–238.

(31) Moore, W. M.; Webber, R. K.; Fok, K. F.; Jerome, G. M.; Kornmeier, C. M.; Tjoeng, F. S.; Currie, M. G. *Bioorg. Med. Chem.* **1996**, *4*, 1559–1564.

(32) Salerno, J. C.; McMillan, K.; Masters, B. S. S. *Biochemistry* **1990**, *33*, 11839–11845.

(33) Moore, W. M.; Webber, R. K.; Jerome, G. M.; Tjoeng, F. S.; Misko, T. P.; Currie, M. G. *J. Med. Chem.* **1994**, *37*, 3886–3888.

(34) Garvey, E. P.; Oplinger, J. A.; Furfine, E. S.; Kiff, R. J.; Laszlo, F.; Whittle, B. J. R.; Knowles, R. G. *J. Biol. Chem.* **1997**, *272*, 4959–4963.

(35) Grant, S. K.; Green, B. G.; Stiffey-Wilusz, J.; Durette, P. L.; Shah, S. K.; Kozarich, J. W. *Biochemistry* **1998**, *37*, 4174–4180.

(36) Bryk, R.; Wolff, D. J. *Biochemistry* **1998**, *37*, 4844–4852.

adducts,<sup>34</sup> and the authors did not propose a mechanism for inactivation.

Structurally more similar to the natural substrate, L-NIO also has demonstrated many of the characteristics of mechanism-based inactivation. Moncada's group reported time-dependent, irreversible (to substrate addition), substrate protectable, and enantiomerically specific inactivation of unpurified iNOS by L-NIO in phagocytic cells.<sup>30</sup> Assays of L-NIO and L-NIL with purified NOS, which show time-dependent inhibition, have been mentioned.<sup>33</sup>

Except for *N*<sup>ω</sup>-methyl-L-arginine<sup>37</sup> and *N*<sup>ω</sup>-allyl-L-arginine,<sup>38</sup> which appear to act by similar mechanisms, the chemical mechanisms for NOS inactivation by any of the other time-dependent NOS inactivators remain obscure. While L-NIO has physicochemical properties similar to those of L-arginine, the same mechanisms for NOS inactivation by *N*<sup>ω</sup>-alkyl-L-arginine analogues cannot be applied, and no mechanisms for the amidino class of NOS inactivators have been proposed to date. Here we report experiments that clarify the product of inactivation of iNOS by L-NIO and suggest possible mechanisms consistent with these results and those of similar amidine-containing inactivators.

## Results

**Spectral Changes during iNOS Inactivation by L-NIO.** L-NIO showed type I binding difference spectra (peak at 390 nm, trough at 430 nm) when used to titrate an iNOS·imidazole complex (see Supporting Information).

**Kinetics of iNOS Inactivation by L-NIO.** When tested for time-dependent inactivation of iNOS, L-NIO showed time-, concentration-, and NADPH-dependent inhibition that was not reversed upon 60-fold dilution into the enzyme assay solution which contained L-arginine in a 2600-fold excess (see Supporting Information). Control incubations do not lose significant amounts of activity over time. Incubations that include an excess of L-arginine do not exhibit time-dependent inactivation. No inactivation by L-NIO was observed when NADP<sup>+</sup> was substituted for NADPH. The rate of NOS inactivation was concentration-dependent, saturable, and had *K*<sub>I</sub> and *k*<sub>inact</sub> values of 13.7 ± 1.6 μM and 0.073 ± 0.003 min<sup>-1</sup>, as determined by the method of Kitz and Wilson,<sup>39</sup> respectively (see Supporting Information). Inactivation by L-NIO also was shown to be irreversible. An inactivated sample was passed through a Penefsky<sup>40</sup> column to separate small molecules from the protein. While a control solution maintained most of its activity, no return of activity was seen with the inactivated sample.

**Heme Loss during Inactivation.** The heme cofactor appears to be involved in the inactivation event. After inactivation, iNOS was passed through a size exclusion column, and a loss in the heme chromophore was observed (Figure 1). The loss of the chromophore also corresponded with the loss of enzyme activity (see Supporting Information). When inactivated NOS samples were subjected to HPLC directly (without prior gel filtration), the area of the peak due to the heme cofactor significantly decreased. Inclusion of catalase in the inactivation mixtures decreased the amount of heme lost in the control solutions but did not eliminate significant loss of heme (47%) in the solutions with L-NIO (see Supporting Information).

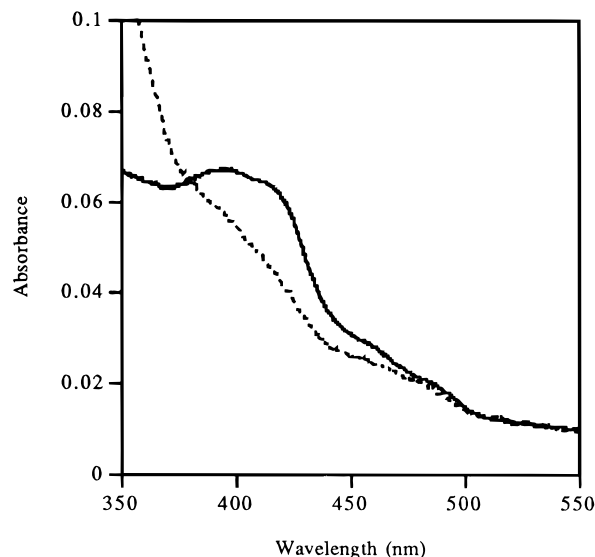
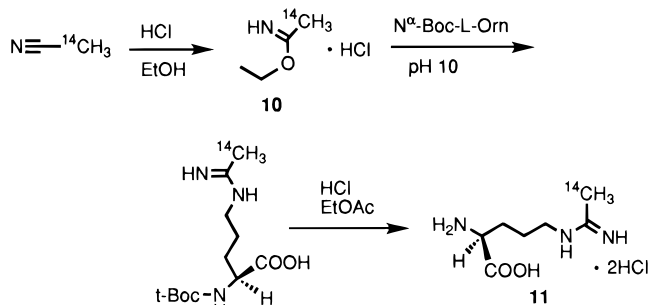


**Figure 1.** Loss of the heme chromophore before ( $t = 0$  h; —) and after inactivation and gel filtration ( $t = 2$  h; - - -). See the Experimental Section for details.

## Scheme 3



***N*<sup>5</sup>-(1-Imino-2-[<sup>14</sup>C]ethyl)-L-ornithine (11).** *N*<sup>5</sup>-(1-Imino-2-[<sup>14</sup>C]ethyl)-L-ornithine (**11**, Scheme 3; [<sup>14</sup>C<sup>ω</sup>]-L-NIO), was synthesized from 2'-[<sup>14</sup>C]acetonitrile via ethyl acetimidate hydrochloride (**10**) as shown in Scheme 3.

**Radioactivity from 11 Bound to iNOS Protein.** To determine if any radioactivity is irreversibly bound to the protein, incubation mixtures were allowed to react and then were subjected to dialysis. No significant radioactivity remained bound to the protein either in incubations containing (42 dpm) or omitting (25 dpm, control) NADPH, indicating that less than 0.01 equiv of inactivator remained bound to the protein and that the remaining radiolabel was released with other small molecules. To rule out the formation of a tight noncovalent association of L-NIO (or a metabolite) with iNOS, an inactivated sample was subjected to Sephadex G-50 chromatography. Protein was observed to elute separately from the radioactivity.

**Radioactivity from 11 Bound to Heme.** To determine if the inactivator is bound to the heme, **11**-inactivated iNOS mixtures were directly chromatographed by HPLC and the elution monitored both by absorbance at 400 nm and by radioactivity. As noted before, significant loss of heme was measured (see Supporting Information). The radiotracer failed to reveal NADPH-dependent formation of a new [<sup>14</sup>C]-labeled peak (see Supporting Information).

**Product Formation during Inactivation of iNOS by 11.** Turnover-dependent production of a [<sup>14</sup>C]-labeled peak with the same retention time as *N*<sup>ω</sup>-hydroxy-L-NIO (**12**; *o*-fluoraldehyde-derivatized) was observed, but no *N*<sup>δ</sup>-acetyl-L-ornithine (**14**) (the small peak at 17 min does not correspond to **14**) or *C*<sup>ω</sup>-hydroxy-

(37) Olken, N. M.; Osawa, Y.; Marletta, M. A. *Biochemistry* **1994**, *33*, 14784–14791.

(38) Zhang, H. Q.; Dixon, R. P.; Marletta, M. A.; Nikolic, D.; Van Breemen, R.; Silverman, R. B. *J. Am. Chem. Soc.* **1997**, *119*, 10888–10902.

(39) Kitz, R.; Wilson, I. B. *J. Biol. Chem.* **1962**, *237*, 3245–3249.

(40) Penefsky, H. *Methods Enzymol.* **1979**, *LVI*, 527.

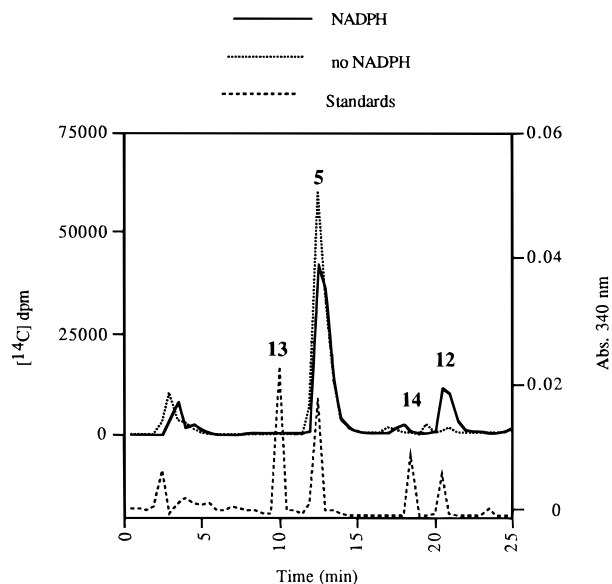
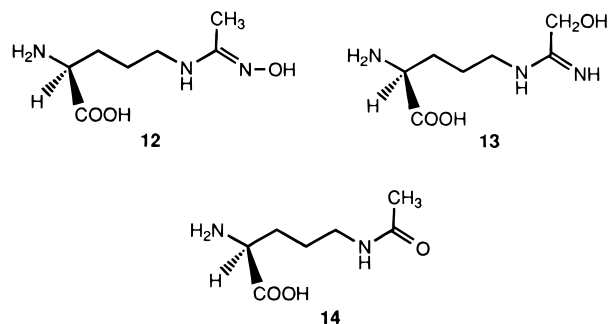


**Figure 2.** Turnover-dependent production of *N*<sup>ω</sup>-hydroxy-L-NIO (**12**) from **11**. Elution times for L-NIO (**5**), *C*<sup>ω</sup>-hydroxy-L-NIO (**13**), and *N*<sup>δ</sup>-acetyl-L-ornithine (**14**) standards are also indicated.



L-NIO (**13**) (Figure 2). When the dpm values from incubations containing NADPH (29 534 dpm) and NADP<sup>+</sup> (6396 dpm) are subtracted, the amount of *N*<sup>ω</sup>-hydroxy-L-NIO (**12**) produced during the inactivation process was calculated to be  $7.7 \pm 0.2$  equiv per inactivation event.

**Inhibition of iNOS by *N*<sup>ω</sup>-Hydroxy-*N*<sup>5</sup>-(1-iminoethyl)-L-ornithine (**12**).** Incubations of **12** with iNOS demonstrated time- and concentration-dependent inactivation that was not reversible upon dilution into the assay solution (see Supporting Information). Incubations that included an excess of L-arginine or with substitution of NADP<sup>+</sup> for NADPH resulted in no significant loss of activity. The  $K_I$  and  $k_{inact}$  values for **12** are  $830 \pm 160$   $\mu$ M and  $0.0073 \pm 0.0007$  min<sup>-1</sup>, respectively.

**Substrate Activity of *N*<sup>ω</sup>-Hydroxy-*N*<sup>5</sup>-(1-iminoethyl)-L-ornithine (**12**).** Using the oxyhemoglobin assay for detection of NO production (see the Experimental Section), **12** was determined to be a substrate for iNOS and showed saturation kinetics with  $K_m$  and  $k_{cat}$  values of  $800 \pm 85$   $\mu$ M and 2.22 min<sup>-1</sup>, respectively. However, **12** was only a poor substrate relative to L-arginine, showing  $k_{cat}/K_m$  values 4 orders of magnitude lower than those of L-arginine (Table 1). The  $k_{cat}$  and  $k_{inact}$  values for **12** can be compared directly to give a partition ratio ( $k_{cat}/k_{inact}$ ) for inactivation of 304; i.e., there are 304 turnovers to give NO per inactivation event.

**Formation of *N*<sup>δ</sup>-Acetyl-L-ornithine (**14**).** Incubations of **12** with iNOS showed NADPH-dependent and time-dependent conversion to **14** (Figure 3).

**Inactivation of iNOS by *N*<sup>δ</sup>-Acetyl-L-ornithine (**14**).** For incubations with iNOS, time-, concentration-, and NADPH-

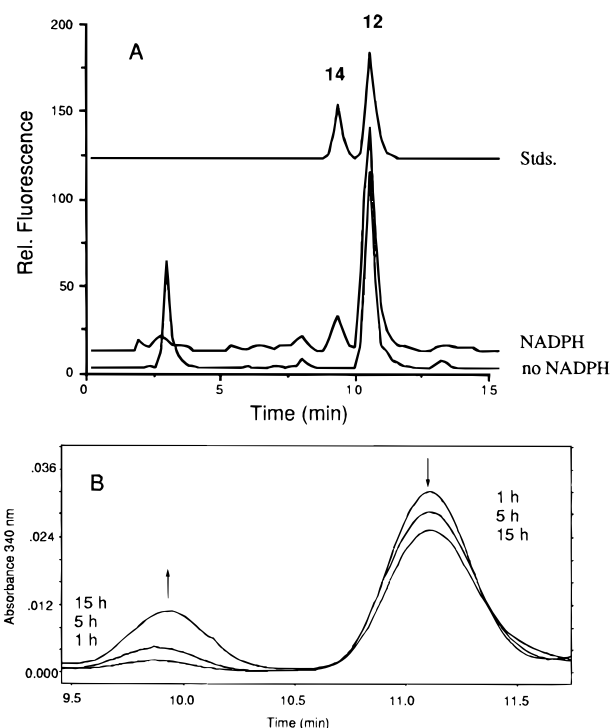


**Figure 3.** Time- and NADPH-dependent production of *N*<sup>δ</sup>-acetyl-L-ornithine (**14**) from *N*<sup>ω</sup>-hydroxy-L-NIO (**12**). (A) The top trace shows retention times for **14** and **12** standards. The middle trace shows an incubation mixture containing **12**, iNOS, and NADPH. The bottom trace shows an identical incubation mixture except without the NADPH. (B) Traces at 1, 5, and 15 h time points of incubations including **12**, iNOS, and NADPH. Due to inactivation, fresh enzyme was added after 5 h and the chromatogram adjusted for the dilution. To shorten run times, the gradient for elution was changed from that in Figure 2, resulting in shorter retention times for **12** and **14** (see the Experimental Section for details).

**Table 1.**  $K_m$  and  $k_{cat}$  Values for L-Arginine and *N*<sup>ω</sup>-Hydroxy-L-NIO (**12**) with iNOS

	L-arginine	<b>12</b>
$K_m$ ( $\mu$ M)	$5.9 \pm 0.5$	$800 \pm 85$
$k_{cat}$ (min <sup>-1</sup> )	84.6	2.22
$k_{cat}/K_m$ ( $\mu$ M <sup>-1</sup> min <sup>-1</sup> )	14.3	$2.8 \times 10^{-3}$

dependent loss of enzyme activity was observed with **14** (see Supporting Information).  $K_I$  and  $k_{inact}$  values for **14** inactivation of iNOS were determined to be 490 mM and 0.24 min<sup>-1</sup>, respectively. iNOS inactivation by **14** can be prevented by including L-arginine, but not D-arginine, in the inactivation mixtures, suggesting that the inactivator acts at the arginine binding site.

**Inhibition of iNOS by *N*<sup>5</sup>-(1-Imino-2-hydroxyethyl)-L-ornithine (**13**).** *C*<sup>ω</sup>-Hydroxy-L-NIO (**13**) failed to cause time-dependent inactivation of iNOS.

**Kinetic Isotope Effect on Inactivation of iNOS by *N*<sup>5</sup>-(1-Imino-2-[C<sup>2</sup>H<sub>3</sub>]ethyl)-L-ornithine (**15**).** Inactivation of iNOS by **15** shows a kinetic isotope effect on  $^Hk_{inact}/^Dk_{inact}$  of  $1.35 \pm 0.08$  ( $0.073 \pm 0.003/0.054 \pm 0.001$ ) and on  $^H(k_{inact}/K_I)/^D(k_{inact}/K_I)$  of  $1.51 \pm 0.3$  ( $5.3 \pm 0.8 \times 10^{-3}/3.5 \pm 0.2 \times 10^{-3}$ ) (see Supporting Information).

**Characterization of Modified Heme.** An enlargement of the HPLC trace after inactivation of iNOS by **5** reveals a new NADPH-dependent peak with absorbance at 400 nm at 47 min (Figure 4). LC-electrospray mass spectrometry was used to

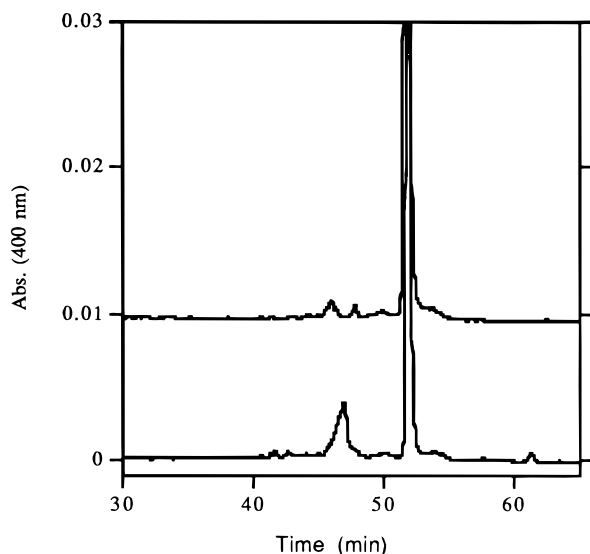


**Figure 4.** HPLC of the NADPH-dependent formation of a new peak (47 min) after inactivation of iNOS by L-NIO.

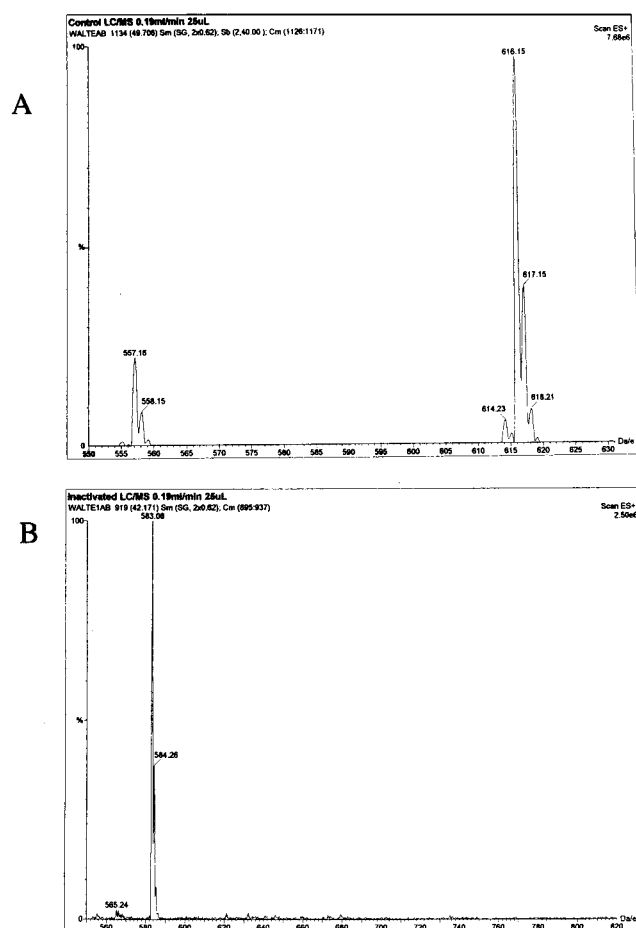


**Figure 5.** Mass spectra of the peaks at 52 min (A) and 47 min (B) in Figure 4.

compare the control (no NADPH) and inactivated (NADPH) mixtures (see Supporting Information). The mass spectra of the peaks in the HPLC trace at 49 min (A) and at 42 min (B) from the inactivated mixture are shown in Figure 5. The ( $m/z$ ) values for the peaks at 49 and 42 min are 616 (heme) and 583, respectively. MS/MS of the 583 peak gave a spectrum (Figure 6A) that was the same as MS/MS of a biliverdin standard (Figure 6B).

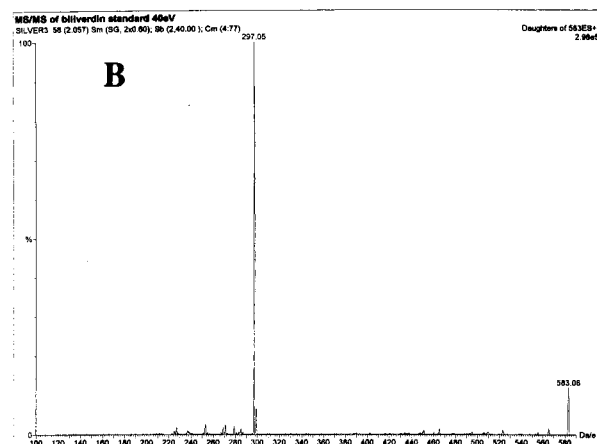
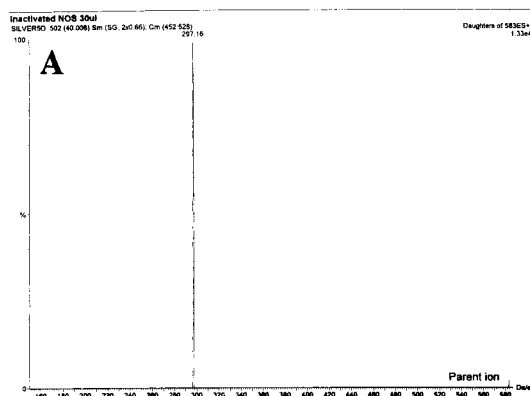
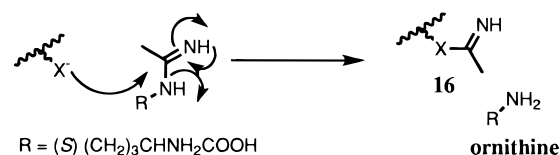


**Figure 6.** (A) MS/MS of the  $m/z$  583 peak in Figure 5B. (B) MS/MS of a biliverdin standard.

#### Scheme 4

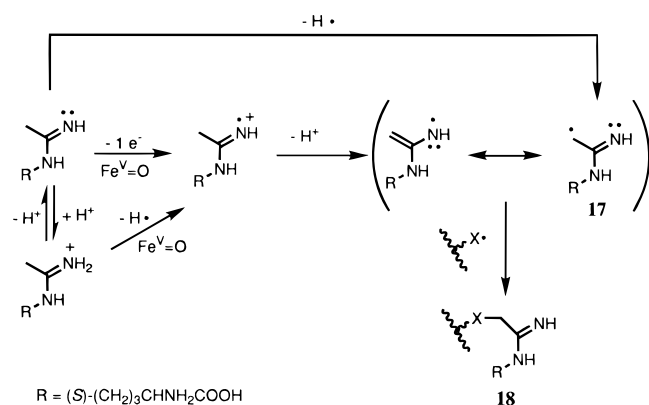


#### Discussion

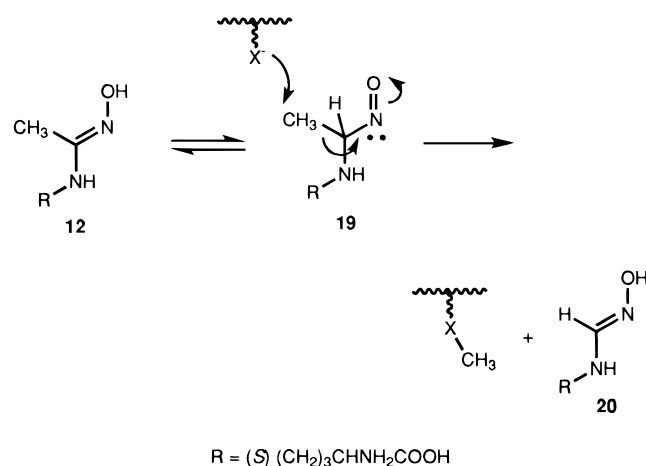
Recently, two reports of the inactivation of NOS by the homologue of L-NIO, namely, L-NIL (**6**), were published.<sup>35,36</sup> Some of the results published are consistent with the results we report here; however, no cause for inactivation nor mechanisms of inactivation were reported. Considering the multistep catalysis by NOS (Scheme 2), there are numerous possibilities for inactivation of NOS by L-NIO at various stages along the catalytic pathway. Inactivation could occur before any oxidation occurs, after a one-electron oxidation, after hydroxylation to yield either **12** or **13**, or at an oxidation state beyond hydroxylation. These possibilities will first be presented, and then experiments designed to differentiate these possibilities will be described and conclusions will be drawn on the basis of these results. Each of these proposed mechanisms has a distinguishing feature that can be determined experimentally. Elucidation of the chemical mechanism of NOS inactivation by L-NIO should provide a paradigm for understanding inactivation by not only L-NIO but also by other amidines.

If inactivation occurs prior to any oxidation (Scheme 4), ornithine would be produced and the enzyme would be modified by imidoylation (**16**); this pathway would not require catalytic turnover by NOS. If inactivation occurs prior to the first hydroxylation step but after initial oxidation, possibly by a high-

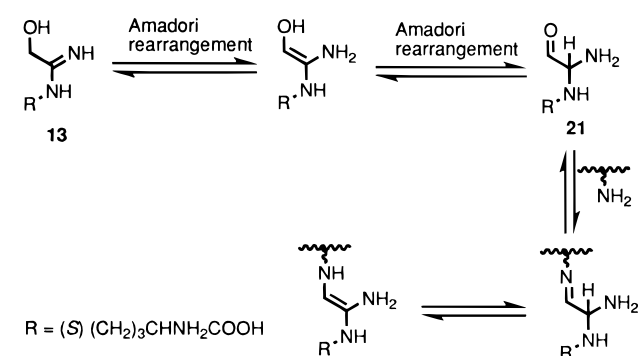
Scheme 5



Scheme 6

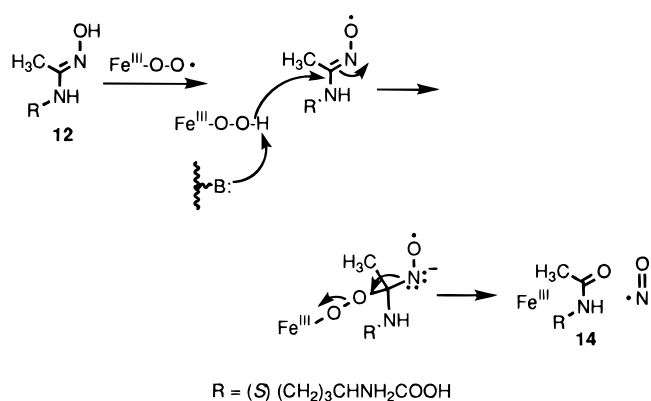


Scheme 7

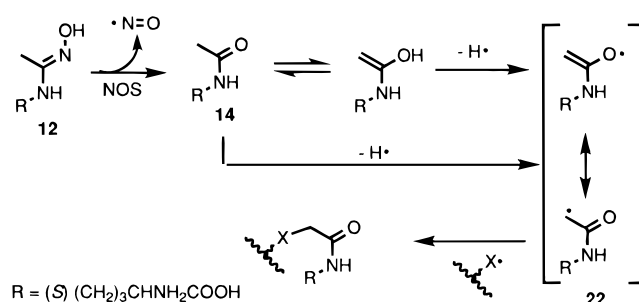


energy iron-oxo or iron-peroxo species (Scheme 5), a radical may be formed at the terminal carbon atom (**17**) by hydrogen atom abstraction directly from the methyl group or from the terminal amidino nitrogen followed by deprotonation; alternatively, **17** could arise from a single electron transfer followed by proton abstraction. The resulting radical could recombine with a cofactor- or enzyme-based radical and result in covalent modification and inactivation (**18**) or may somehow uncouple peroxide formation. If the inactivation event occurs after the initial hydroxylation, as it does for both *N*<sup>ω</sup>-methyl-L-arginine<sup>37</sup> and *N*<sup>ω</sup>-allyl-L-arginine,<sup>38</sup> either the terminal amidino nitrogen (Scheme 6) or carbon (Scheme 7) positions may be hydroxylated. Oxidation of amidino nitrogens<sup>18a</sup> and unactivated carbons<sup>19</sup> have both been shown to be catalyzed by cytochrome P450 enzymes. Isomerization of **12** to nitroso **19** (Scheme 6) may inhibit the enzyme by coordination to the heme; nitroso- (Fe<sup>II</sup>) heme complexes are very stable and can result in pseudo-

Scheme 8



Scheme 9



irreversible enzyme inhibition.<sup>41</sup> Alternatively, the nitroso compound may also be attacked by a cofactor or enzyme based nucleophile, resulting in methylation of the attacking group and release of the amidoxime (**20**). Both of these pathways should not require turnover by NOS after the initial *N*<sup>ω</sup>-hydroxylation. An Amadori rearrangement of C-hydroxylated L-NIO (**13**; Scheme 7) would give an aldehyde (**21**) that could form a Schiff base with a lysine residue and lead to enzyme inactivation.

It also is possible that **12** may serve as an alternative substrate for NOS, producing NO and **14** (Scheme 8). Production of nitric oxide would require O<sub>2</sub> and NADPH, even after the initial formation of **12**. Inactivation pathways also can be proposed that require further oxidation of **14** (Scheme 9). Hydrogen atom abstraction of the methyl group or of the enol gives an α-radical (**22**) that could combine with either a cofactor or protein-based radical or somehow uncouple peroxide formation, just like the corresponding L-NIO radical (Scheme 5). This pathway should require enzymatic turnover after the initial *N*<sup>ω</sup>-hydroxylation and turnover after formation of **14**. The potential mechanisms in Schemes 4–9 were tested as described below.

L-NIO shows type I binding difference spectra when used to titrate an iNOS·imidazole complex (data not shown). These spectra are very similar to those exhibited by titrations of rat nNOS with L-arginine, *N*<sup>ω</sup>-methyl-L-arginine, or *N*<sup>ω</sup>-hydroxy-L-arginine<sup>42</sup> and dissimilar to the type II difference spectra seen with imidazole and L-thiocitrulline.<sup>43</sup> The observation of type I difference spectra indicates that L-NIO binds in a manner similar to that of arginine and is capable of inducing similar changes in the heme environment (a shift toward a high-spin pentacoordinate ferric species), supporting the possibility that L-NIO binds, and may be oxidized, in a manner similar to that of the normal substrate.

(41) Mansuy, D.; Gans, P.; Chottard, J.; Bartoli, J. *Eur. J. Biochem.* **1988**, *76*, 607–615.

(42) McMillan, K.; Masters, B. S. S. *Biochemistry* **1993**, *32*, 9875–9880.

(43) Frey, C.; Narayanan, K.; McMillan, K.; Spak, L.; Gross, S. S.; Masters, B. S.; Griffith, O. W. *J. Biol. Chem.* **1994**, *269*, 26083–26091.

When tested for time-dependent inactivation of iNOS, L-NIO shows time-, concentration-, and NADPH-dependent inhibition that is not reversed by dilution into the enzyme assay solution containing L-arginine in a 2600-fold excess or by passing through a Penefsky<sup>40</sup> column to separate small molecules from the protein (data not shown). This type of saturation kinetics is consistent with a requirement for enzymatic processing of a latent inactivator, as proposed in most of the mechanisms above. L-Arginine blocks the inactivation by L-NIO, reinforcing the proposal that both L-NIO and L-arginine compete for the same binding site. However, no inactivation by L-NIO was observed when NADP<sup>+</sup> was substituted for NADPH, indicating that an oxidation is required for inactivation to occur. The O<sub>2</sub> dependence for inactivation NOS by L-NIL was noted earlier.<sup>35</sup> Because NADPH is required for loss of activity, a simple transamidation inactivation mechanism, such as shown in Scheme 4, is not reasonable. This is in agreement with the crystal structure of iNOS,<sup>5</sup> which indicates that reactive nucleophiles are not present near the guanidinium binding site.

The heme cofactor appears to be involved in the inactivation event, as evidenced by the change in both the visible spectrum (Figure 1) and by HPLC (data not shown). Loss of about 50% of the heme chromophore following inactivation and gel filtration indicates that the heme has either dissociated intact from the enzyme or that it is modified or destroyed during inactivation. The loss of the heme chromophore corresponds with the loss of enzyme activity (data not shown). These experiments suggest that cofactor loss is involved in the inactivation process but do not distinguish between heme modification or destruction and heme release without modification (possibly due to disruption of the active iNOS homodimer into inactive monomers). When inactivated NOS samples were subjected to HPLC directly (without prior gel filtration), the area of the peak due to the heme cofactor significantly decreased, indicating that heme is either modified or destroyed during inactivation and not just dissociated intact from the active homodimer. Inclusion of catalase in the inactivation mixtures decreased the amount of heme lost in the control solutions but did not eliminate significant loss of heme (47%) in the solutions with L-NIO. This rules out the possibility that heme loss is due solely to uncoupled peroxide production<sup>44</sup> and reinforces the proposal of inactivator-mediated heme destruction. Modification of only about half of the heme cofactor probably results from either half sites reactivity or from disruption of the active iNOS homodimer into inactive monomers; heme has been shown to be essential for iNOS dimer formation.<sup>45</sup> Inactivation of iNOS by L-NIL also gives incomplete loss of heme<sup>35,36</sup> with a concomitant shift of the dimer/monomer population to predominantly monomer.<sup>36</sup>

N<sup>5</sup>-(1-Imino-2-[<sup>14</sup>C]ethyl)-L-ornithine (**11**, Scheme 3) was synthesized to determine if and where the inactivator becomes attached to the enzyme. After inactivation, no significant radioactivity remained bound to the protein either in the presence or absence of NADPH. This is consistent with similar studies using radiolabeled L-NIL.<sup>35,36</sup> To rule out the formation of a tight noncovalent association of L-NIO (or a metabolite) with iNOS, a sample inactivated with **11** was subjected to gel filtration. Protein was observed to elute separately from the radioactivity, indicating that inactivator does not bind to the protein. To determine if the inactivator is bound to the heme, **11**-inactivated iNOS mixtures were directly chromatographed

by HPLC and the elution was monitored both by absorbance at 400 nm and by radioactivity. About half of the heme ( $t = 52$  min) was lost, and no radioactivity was observed in the chromatogram at or near the heme peak. This indicates that the inactivator does not covalently bond to released molecules (e.g., cofactors) or to the protein.

Possibly L-NIO is metabolized by iNOS to a product that is responsible for inactivation. NADPH-dependent production of a [<sup>14</sup>C]-labeled peak with the same retention time as *N*<sup>ω</sup>-hydroxy-L-NIO (**12**; *o*-phthalaldehyde-derivatized) was observed, indicating that the terminal amidino nitrogen can be hydroxylated by iNOS (Figure 2); the amount produced corresponds to  $7.7 \pm 0.2$  equiv per inactivation event, a rather low partition ratio. Neither *N*<sup>δ</sup>-acetyl-L-ornithine (**14**; *o*-phthalaldehyde-derivatized) nor *C*<sup>ω</sup>-hydroxy-L-NIO (**13**) was detected as a product.

Incubation of **12** with iNOS produced time-, concentration-, and NADPH-dependent inactivation that was not reversed upon dilution into the assay solution. Incubations that included an excess of L-arginine or with substitution of NADP<sup>+</sup> for NADPH resulted in no significant loss of activity, demonstrating substrate-protectable and turnover-dependent inactivation, respectively, similar to that seen earlier with L-NIO. These results suggest that isomerization of **12** to the nitroso species **19** (Scheme 6) or direct reaction of **19** with the enzyme is unlikely because inactivation by **12** requires additional reducing equivalents from NADPH for loss of activity.

It might, at first, be tempting to conclude that NOS inactivation by L-NIO is caused by *N*<sup>ω</sup>-hydroxylation to **12**, followed by enzyme inactivation; however, the  $K_I$  and  $k_{\text{inact}}$  values for **12**, 830 μM and 0.0073 min<sup>-1</sup>, respectively, indicate that any inactivation by L-NIO which proceeds via **12** can only account for less than 10% of the total inactivation because the  $K_I$  value for L-NIO ( $13.7 \pm 1.6$  μM) indicates that L-NIO binds about 60 times more tightly to NOS than does **12**, and the  $k_{\text{inact}}$  value for L-NIO ( $0.073 \pm 0.003$  min<sup>-1</sup>) is 10 times greater than that for **12** (the  $k_{\text{inact}}/K_I$  for L-NIO is 3 orders of magnitude greater than that for **12**). Therefore, **12** is not a kinetically competent intermediate. Although **12** is, at most, a minor contributor to inactivation by L-NIO, at high concentrations it can serve as a substrate for iNOS, exhibiting saturation kinetics with  $K_m$  and  $k_{\text{cat}}$  values of  $800 \pm 85$  μM and 2.22 min<sup>-1</sup>, respectively (Table 1). As predicted by Scheme 8, concomitant production of **14** is also observed in an NADPH- and time-dependent manner (Figure 3). Since the  $K_m$  and  $K_I$  values for **12** are the same, the  $k_{\text{cat}}$  and  $k_{\text{inact}}$  values can be compared directly to give a partition ratio for inactivation ( $k_{\text{cat}}/k_{\text{inact}}$ ) of 304. This provides further evidence that during inactivation by L-NIO, **12** is not an intermediate and is released into solution without further processing. If even 10% of the inactivation proceeded through **12**, then a significant amount of **14** would have been produced; however, none was detected (Figure 2). Because of its high  $K_m$  value compared with that of L-NIO, it is unlikely that any **12** released into solution could compete with L-NIO for rebinding and further turnover by iNOS.

Considering that inactivation does not proceed from **12**, a mechanism involving *C*<sup>ω</sup>-hydroxylation was considered. *C*<sup>ω</sup>-Hydroxy-L-NIO (**13**) failed to cause time-dependent inactivation of iNOS, which rules out the inactivation pathways proposed that occur after *C*<sup>ω</sup>-hydroxylation (e.g., see Scheme 7). NOS does not appear to be restrictive against binding hydroxylated catalytic intermediates. For example, *N*<sup>ω</sup>-hydroxyarginine,<sup>15</sup> *N*<sup>ω</sup>-hydroxy-*N*<sup>ω</sup>-methylarginine,<sup>15</sup> and *N*<sup>ω</sup>-hydroxy-*N*<sup>ω</sup>-allylarginine<sup>38</sup> are all examples of hydroxylated intermediates that are accepted and processed in a kinetically competent manner by NOS.

(44) Heinzl, B.; John, M.; Klatt, P.; Bohme, E.; Mayer, B. *Biochem. J.* **1992**, *281*, 627–630.

(45) Baek, K. J.; Thiel, B. A.; Lucas, S.; Stuehr, D. J. *J. Biol. Chem.* **1993**, *268*, 21120–21129.



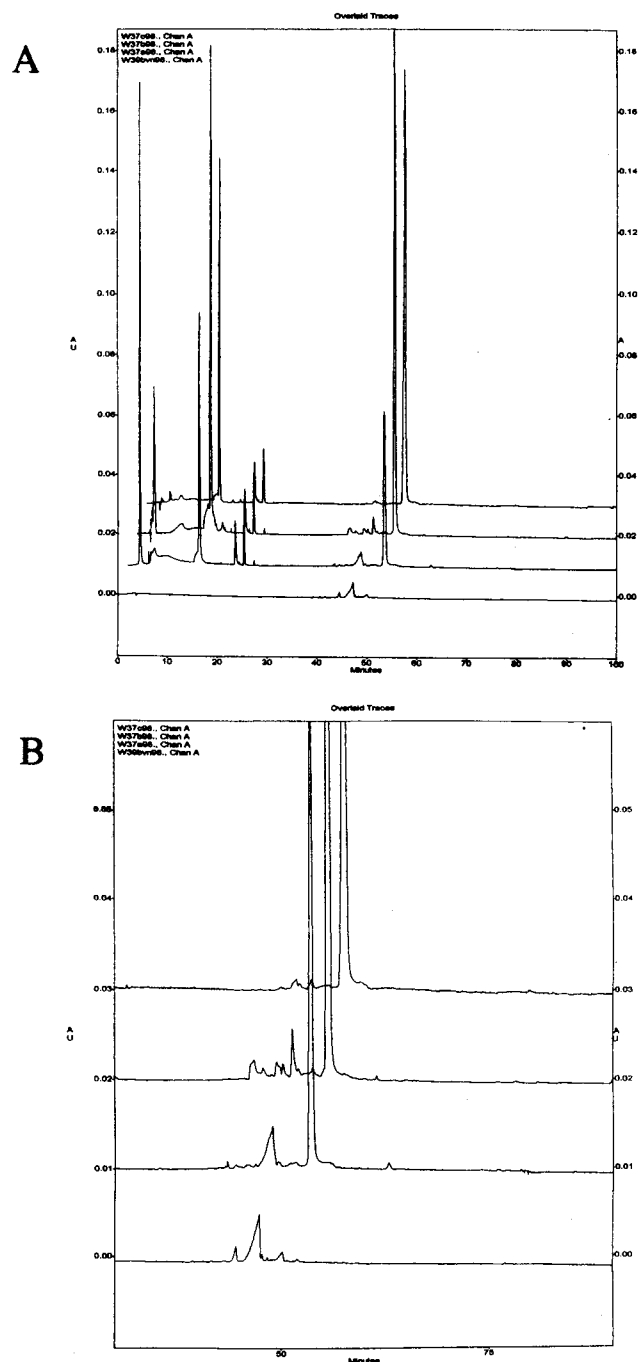


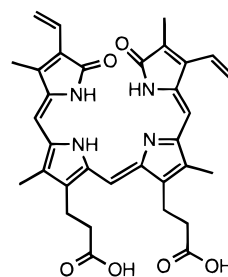
**Figure 7.** Heme loss requiring both NADPH and L-NIO. (A) HPLC chromatograms of iNOS and catalase incubation mixtures containing (from top to bottom) L-NIO only, NADPH only, L-NIO and NADPH, and a biliverdin standard. For easier viewing of heme loss ( $t = 52$  min), the retention times for all three experiments are offset by 2 min from the previous experiment. (B) An expanded view of (A) between 30 and 80 min.

Since neither  $N^{\omega}$ -hydroxy-L-NIO (**12**) nor  $C^{\omega}$ -hydroxy-L-NIO (**13**) is responsible for inactivation of iNOS by L-NIO, and oxidation (NADPH) is required for inactivation, the inactivation must precede the hydroxylation step but follow an oxidation step. This precludes the mechanism shown in Scheme 9 (via Scheme 8) from being relevant. The only mechanism presented that is consistent with these requirements is the one in Scheme 5; however, it was shown that radioactive L-NIO does *not* become bound to either the protein or to a cofactor, which would be inconsistent with structure **18**. If this mechanism is correct, then it means that either the radical generated by hydrogen atom

abstraction (or electron transfer–proton transfer) of L-NIO is involved in heme destruction without attachment to it or that, if attachment does occur, it is only the first step in a process that eventually releases this radical from the heme.

To determine if either of these proposals based in Scheme 5 is reasonable, an experiment was carried out to determine if methyl C–H bond cleavage is involved in the inactivation process. In fact, a kinetic isotope effect on inactivation of iNOS by  $N^5$ -(1-imino-2- $[C^2H_3]$ ethyl)-L-ornithine (**15**,  $d_3$ -L-NIO) ( $^Hk_{\text{inact}}/^Dk_{\text{inact}}$  of  $1.35 \pm 0.08$ ;  $^H(k_{\text{inact}}/K_I)/^D(k_{\text{inact}}/K_I)$  of  $1.51 \pm 0.3$ ) was observed. Although the isotope effects on  $k_{\text{inact}}$  and  $k_{\text{inact}}/K_I$  are small, they are significant and not uncommonly small for primary isotope effects observed in other enzymatic reactions.<sup>46</sup> They are also similar in magnitude to isotope effects observed on inactivation rates for deuterated mechanism-based inactivators of other enzymes. For example, a keto–enol tautomerism of an  $\alpha$ -chloro ketone was proposed in an inactivation mechanism for UDP galactose-4-epimerase and was supported with an isotope effect on  $k_{\text{inact}}$  of 1.4 ( $^Hk_{\text{inact}}/^Dk_{\text{inact}}$ ).<sup>47</sup> Also, an  $N$ -methyl mechanism-based inactivator of cytochrome P450 demonstrated a  $k_{\text{inact}}$  isotope effect of 2 when a trideuteriomethyl group was substituted.<sup>48</sup> The observation of a primary kinetic isotope effect on NOS inactivation by L-NIO suggests that C–H bond scission is a partially rate-determining step in the inactivation mechanism, and this is consistent with the first step in the inactivation mechanism proposed in Scheme 5.

The conundrum, based on the mechanism in Scheme 5, of having no inactivator bound to either protein or to the heme is discussed below, but first the question of what the heme is converted into is considered. From Figure 4 it is apparent that a new NADPH-dependent peak in the HPLC chromatogram at about 47 min (400 nm) results from L-NIO inactivation of NOS. LC–electrospray mass spectrometry was carried out to identify the masses of the peaks at 47 and 52 min. The peak at 52 min has a  $m/z$  value (Figure 5A) of 616 and corresponds to unmodified heme. The peak at 47 min has a  $m/z$  value (Figure 5B) of 583, which is consistent with the mass of the heme degradation product biliverdin IX (**23** shows biliverdin IX $\alpha$ , that



**23**

is, oxidative cleavage at the  $\alpha$ -*meso* carbon). MS/MS of this product (Figure 6A) was the same as that for a biliverdin standard (Figure 6B). Formation of biliverdin requires oxidative cleavage of the heme macrocycle to a linear tetrapyrrole and loss of a *meso* carbon.

To rule out L-NIO independent heme destruction caused only by the presence of NADPH (and subsequent enzymatic formation of an oxidant), incubations of iNOS and catalase containing L-NIO only, NADPH only, or L-NIO and NADPH were compared with a biliverdin standard (Figure 7). Only the

(46) Klinman, J. P. *Adv. Enzymol.* **1978**, *46*, 415–494.

(47) Flentke, G. R.; Frey, P. A. *Biochemistry* **1990**, *29*, 2430–2436.

(48) Kunze, K. L.; Trager, W. F. *Chem. Res. Toxicol.* **1993**, *6*, 649–656.

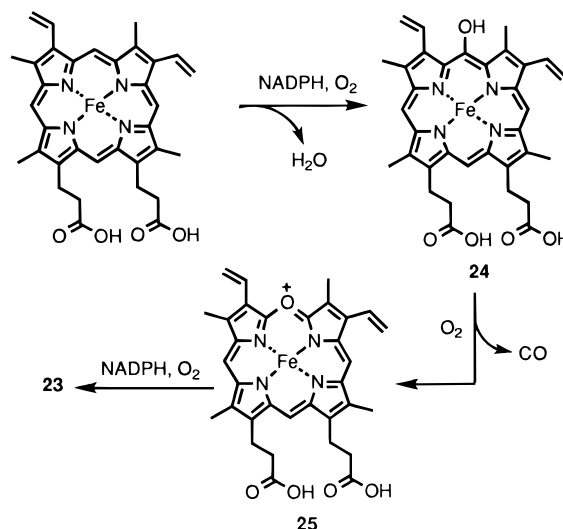
incubation containing both NADPH and L-NIO showed significant loss of heme and formation of a biliverdin peak at 47 min. Thus, the presence of L-NIO is mandatory for heme destruction. The peak area for biliverdin (at 400 nm) varies with concentration in a linear manner over the concentrations detected in the inactivation solutions. On the basis of these standards, the average peak area of three separate inactivations indicates that  $0.63 \pm 0.1$  equiv of biliverdin is produced per inactivation event, which corresponds to the loss of about half of the heme from the UV-vis and HPLC experiments described above.

Simple peroxide formation also cannot be the cause for heme degradation to biliverdin. Peroxide, produced both enzymatically (NADPH-P450 reductase, NADPH, and O<sub>2</sub>) and nonenzymatically, is known to degrade free heme and cytochrome P450 bound heme.<sup>49</sup> Initially, it was reported that biliverdin is a very small (3–14%) byproduct of heme degradation;<sup>50,51</sup> however, the major products of peroxidative heme cleavage were later shown<sup>49</sup> to consist of various propentdyopents, maleimides, formic acid (the *meso* carbons), and hematinic acid, and biliverdin was shown *not* to be an intermediate in this process.

Peroxyxynitrite is known to inactivate iNOS, possibly by an oxidation of the heme thiolate ligand.<sup>52</sup> However, peroxyxynitrite cannot be responsible for inactivation by L-NIO because no nitric oxide (which reacts with superoxide to give peroxyxynitrite) is produced from L-NIO. Nitric oxide is produced from *N*-hydroxy-L-NIO (**12**), but thiols have a protective effect,<sup>52</sup> and the inactivation studies were carried out in the presence of 10 mM dithiothreitol and catalase (100–1000 units). Furthermore, it was shown that only about 8 equiv of **12** are generated during inactivation and are not further processed. Therefore, it is doubtful that peroxyxynitrite is responsible for inactivation by L-NIO.

A summary of the data describing the inactivation of iNOS by L-NIO is as follows: complete inactivation converts approximately half of the heme cofactor to biliverdin, does not covalently modify the protein, does not proceed through C<sup>ω</sup>-hydroxylation, releases a small amount of the N<sup>ω</sup>-hydroxylation product as a turnover product, and exhibits a kinetic isotope effect upon substitution of L-NIO with d<sub>3</sub>-L-NIO. On the basis of these experimental results, at least two reasonable, but speculative, mechanisms for the inactivation by L-NIO can be proposed. In the first mechanism, L-NIO serves to disrupt the normal redox cycle of NOS following one-electron oxidation, possibly by shifting the heme spin state, increasing uncoupled peroxide production, and altering the heme environment, thereby resulting in oxidative cleavage of the heme macrocycle to biliverdin IX. Our results indicate that catalase does not prevent inactivation, but that result only supports the notion that excess peroxide from solution is not responsible for inactivation. It does not preclude a mechanism in which some of the hydrogen peroxide generated at the active site causes heme destruction prior to release into solution. It is known that biliverdin is produced by the enzyme heme oxygenase,<sup>53</sup> an enzyme that cleaves the α-*meso* bridge of the heme regiospecifically, proceeding through α-*meso*-hydroxyheme (**24**) and verdoheme (**25**) as intermediates, liberating the *meso* carbon as carbon monoxide, and leaving biliverdin IXα (**23**) as the product

Scheme 10



(Scheme 10).<sup>53,54</sup> The proposal that L-NIO causes uncoupled peroxide production is consistent with the idea of substrate-assisted catalysis<sup>5,21</sup> in the first oxidation step in which the proton of the terminal NH<sub>2</sub> group of L-arginine provides the catalysis for conversion of peroxoheme to the purported Fe<sup>V</sup>=O species. L-NIO, however, does not have the terminal NH<sub>2</sub> group to deliver a proton to peroxoheme, so that leaves the heme-based oxidant in the peroxo state, possibly resulting in the production of excess peroxide.

In a second proposed mechanism, L-NIO is oxidized initially by one of the pathways in Scheme 5, where X is the heme. The partitioning between turnover and inactivation occurs with C–H bond cleavage. If L-NIO is bound in a manner similar to that of aminoguanidine<sup>21</sup> or L-arginine<sup>5</sup> and orients the amidino nitrogen toward the heme (for electron transfer), glutamate 371 would be correctly positioned to abstract a proton from the terminal methyl group of (one-electron oxidized) L-NIO, producing **17** (Scheme 5). Alternatively, if L-NIO was bound with the terminal methyl group pointing toward the heme, it would be correctly placed for heme peroxo abstraction of a hydrogen atom directly from the carbon to give **17** (Scheme 5). Formation of L-NIO–heme adduct **26** (equivalent to **18**, X = heme, in Scheme 5) is proposed to initiate a rapid series of reactions leading to the formation of biliverdin and regenerating L-NIO, as depicted in Scheme 11 (α-*meso*-alkylation is arbitrary; it could alkylate at any of the *meso*-positions). The conversion of alkylheme **26** to biliverdin (**23**) and L-NIO shown in Scheme 11 is similar to the mechanism proposed by Ortiz de Montellano and co-workers<sup>55</sup> for the heme oxygenase-dependent conversion of α-*meso*-methylheme to biliverdin. According to this mechanism, the α-*meso*-alkyl heme is first converted to the heme hydroperoxide (**27**) followed by protonation and electrophilic substitution at the α-*meso* carbon to give cation **28**. A two-electron reduction of O<sub>2</sub> leads to formation of peroxide **29**, which breaks down by homolytic cleavage of the O–O and C–C bonds to give **30**. In the case of α-*meso*-methylheme, the fate of the methyl and α-*meso* carbon is not known although verdoheme was detected as an intermediate.<sup>54</sup> In our case, we also propose the formation of verdoheme (**25**), possibly via **31** in addition to C<sup>ω</sup>-carboxy-L-NIO (**32**), which should undergo rapid decarboxylation and release unmodified L-NIO. This would account

(49) Schaefer, W. H.; Harris, T. M.; Guengerich, F. P. *Biochemistry* **1985**, *24*, 3254–3263.

(50) Guengerich, F. P. *Biochemistry* **1978**, *17*, 3633–3639.

(51) Docherty, J. C.; Masters, B. S. S.; Firneisz, G. D.; Schacter, B. A. *Biochem. Biophys. Res. Commun.* **1982**, *105*, 1005–1013.

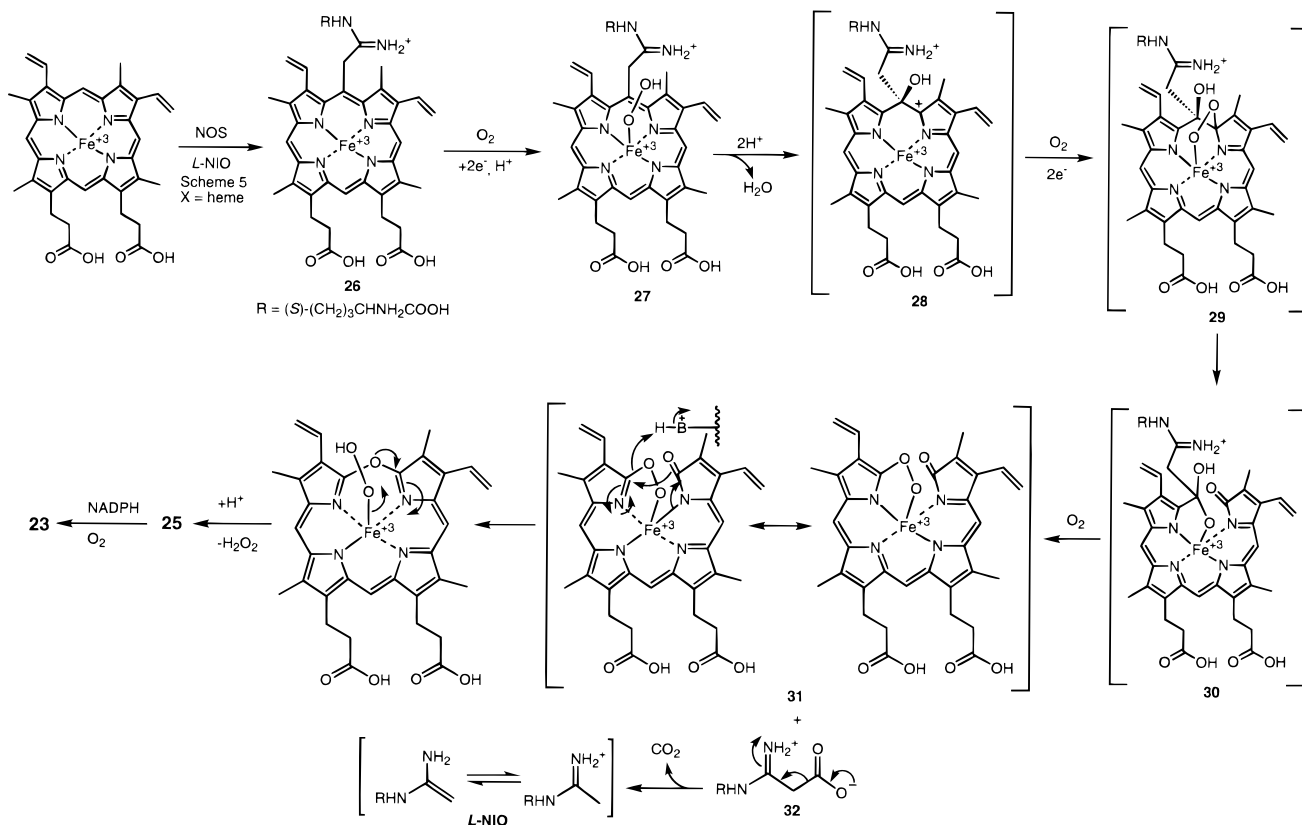
(52) (a) Humer, A. F. R.; Nishida, C. R.; Ortiz de Montellano, P. R.; Schoneich, C. *Chem. Res. Toxicol.* **1997**, *10*, 618–626. (b) Pasquet, J. P. E. E.; Zou, M. H.; Ullrich, V. *Biochimie* **1996**, *78*, 785–791.

(53) (a) Maines, M. D. *FASEB J.* **1988**, *2*, 2557–2568. (b) Tenhunen, R.; Marver, H. S.; Schmid, R. *J. Biol. Chem.* **1969**, *244*, 6388–6394.

(54) Torpey, J.; Ortiz de Montellano, P. R. *J. Biol. Chem.* **1996**, *271*, 26067–26073.

(55) Torpey, J.; Lee, D. A.; Smith, K. M.; Ortiz de Montellano, P. R. *J. Am. Chem. Soc.* **1996**, *118*, 9172–9173.

Scheme 11



for why no radiolabeled adduct or modified amino acids (other than **12**) were detected. The verdoheme (**25**) produced could then be converted to biliverdin corresponding to the reaction catalyzed by heme oxygenase. Although heme oxygenase catalyzes destruction of both heme and alkylated hemes, this proposal suggests that, in the case of NOS, only after heme alkylation does the enzyme initiate a reaction similar to that of heme oxygenase. It is not known if the biliverdin resulting from NOS inactivation by L-NIO consists of a single isomer or a mixture of isomers. Because no L-NIO–biliverdin adducts were isolated, heme cleavage must occur at the point of inactivator attachment and not at an unsubstituted *meso* carbon, consistent with the work of Ortiz de Montellano and co-workers.<sup>55</sup>

This second proposed inactivation mechanism is significant for several reasons. The similarities between L-NIO and the usual substrate, L-arginine, suggest that NOS may use the normal catalytic mechanism to process both of these compounds. While previously studied mechanism-based inactivators of NOS target the second oxidation step, the oxidation of *N*<sup>ω</sup>-hydroxy-L-arginine to citrulline and NO,<sup>38</sup> L-NIO would be the first known probe of the first step, the hydroxylation of L-arginine to *N*<sup>ω</sup>-hydroxy-L-arginine. A standard heme [Fe<sup>V</sup>=O] species is usually invoked in mechanisms for the first oxidation step, but this proposal has been based largely on similarities to P450 type chemistry, X-ray crystal structures, and on partial CO inhibition and lacks rigorous chemical evidence for a heme-based rather than a tetrahydrobiopterin-based oxidant. Formation of an L-NIO heme adduct, albeit unstable, would be indicative of a heme-based radical providing more compelling evidence as to the identity of the actual oxidant. It remains unclear as to why the reported allyl–heme adduct<sup>38</sup> is further reduced, whereas this L-NIO–heme adduct is further oxidized; perhaps the *N*-hydroxy-*N*-allylarginine intermediate blocks productive O<sub>2</sub> binding to the heme iron, so the electrons meant for the O<sub>2</sub> are transferred to the heme instead.

To complete the picture of the metabolism of L-NIO by iNOS, we investigated the further reaction of **12**, which, as noted above, does not appear to be involved in inactivation of iNOS. Since NO is produced from **12** (the assay for substrate activity of **12** was to monitor the conversion of oxyhemoglobin to methemoglobin by NO), then as shown in Scheme 8, concomitant production of *N*<sup>δ</sup>-acetyl-L-ornithine (**14**) also should be observed. Oxidation of **12** to NO and **14** is observed only at high concentrations of **12**. Incubations of iNOS with **12** led to a NADPH- and time-dependent conversion to **14** (Figure 3). Interestingly, when **14** was incubated with iNOS, time-, concentration-, and NADPH-dependent loss of enzyme activity also was observed; the *K*<sub>I</sub> and *k*<sub>inact</sub> values for **14** inactivation of iNOS were determined to be 490 mM and 0.24 min<sup>-1</sup>, respectively. The *K*<sub>I</sub> value for **14** is quite high, probably reflecting the loss of affinity due to the lack of a guanidinium or amidinium ion. iNOS inactivation by **14** can be prevented by inclusion of L-arginine, but not D-arginine, in the inactivation mixtures, suggesting that the inactivator acts at the arginine binding site. While the *K*<sub>I</sub> for this compound is very large (too large to be relevant to the inactivation by L-NIO), **14** is still of interest because it provides another example of a nonguanidino, neutral side chain, amino acid inhibitor of NOS. This type of compound will presumably be transported by a neutral transporter (perhaps the same as citrulline<sup>29</sup>) and, therefore, should be clinically interesting as a lead compound for use in conjunction with arginine transporter inhibitors in combination therapy, which could target both NO production by NOS and arginine delivery by the γ<sup>+</sup> transporter.

## Experimental Section

**General Methods and Reagents.** Optical spectra and enzyme assays were recorded on a Perkin-Elmer Lambda 10 UV/vis spectrophotometer. NMR spectra were recorded on a Varian Gemini-300 300 MHz

instrument. Chemical shifts are reported as  $\delta$  values in parts per million downfield from Me<sub>4</sub>Si as the internal standard in CDCl<sub>3</sub>, unless stated otherwise. Mass spectra were recorded on a VG Instruments VG70-250SE high-resolution spectrometer. LC-electrospray ionization mass spectra were obtained with a Hewlett-Packard series 1050 HPLC coupled to a Micromass Quattro II triple quadrupole electrospray mass spectrometer. Melting points were obtained with a Fisher-Johns melting point apparatus and are uncorrected.

*N*<sup>α</sup>-Boc-L-ornithine was purchased from either Bachem Bioscience Inc. (King of Prussia, PA) or ICN Pharmaceuticals Inc. (Costa Mesa, CA). *N*<sup>α</sup>-Boc-*N*<sup>β</sup>-Cbz-L-ornithine, NADPH, HEPES, DTT, calmodulin, and human ferrous hemoglobin were purchased from Sigma Chemical Co. Tetrahydrobiopterin (BH<sub>4</sub>) was obtained from B. Schircks Laboratories (Jona, Switzerland) or from Alexis Biochemicals (San Diego, CA). *tert*-Butyl alcohol was purchased from Mallinckrodt. D<sub>2</sub>O was purchased from Cambridge Isotope Laboratories, and CDCl<sub>3</sub> was purchased from Aldrich Chemical Co. Acids, bases, and conventional organic solvents were purchased from Fisher. DCC, DMAP, 10% Pd/C, ethanol-*d*, acetonitrile-*d*<sub>3</sub>, and acetyl chloride were purchased from Aldrich. TLC plates (silica gel 60-F254, 250 μM), and silica gel 60 (230–400 mesh) were purchased from VWR Scientific.

***N*<sup>5</sup>-(1-Iminoethyl)-L-ornithine (L-NIO, 5).** This compound was either purchased as the hydrochloride salt from Research Biochemicals International (Natick, MA) or was synthesized as the dihydrochloride salt by literature methods (0.81 mmol, 38%).<sup>33</sup> <sup>1</sup>H NMR (D<sub>2</sub>O)  $\delta$  1.6–2.1 (m, 4 H), 2.15 (s, 3 H), 3.25 (t, 2 H), 4.06 (t, 1 H); <sup>13</sup>C NMR (D<sub>2</sub>O)  $\delta$  22.47, 26.66, 30.98, 45.29, 56.40, 66.5 (dioxane), 168.82, 175.60; M·H<sup>+</sup><sub>obs</sub> = 174.1267, M·H<sup>+</sup><sub>calcd</sub> = 174.1243.

***N*<sup>5</sup>-(1-Imino-2-[<sup>14</sup>C]ethyl)-L-ornithine ([<sup>14</sup>C<sup>ω</sup>]-L-NIO, 11).** Three aliquots of cold EtOH saturated with HCl(g) were used to wash 2.5 μL of [<sup>14</sup>CH<sub>3</sub>CN (21 mCi/mmol; Sigma) from an ampule cooled in a CCl<sub>4</sub>/CO<sub>2</sub>(s) bath into a tared Wheaton vial. Unlabeled CH<sub>3</sub>CN (21 μL) was added, and the vial was capped and stirred on ice for 0.5 h and then at room temperature for 15 h. The resulting ethyl acetimidate·HCl salt (**10**) was precipitated with addition of cold Et<sub>2</sub>O, the remaining solution removed with a pipet, and the solid dried with a stream of N<sub>2</sub>(g). The solid was washed three times with Et<sub>2</sub>O and then dried under vacuum for 3 h (56.9 mg, 0.46 mmol). *N*<sup>α</sup>-Boc-L-ornithine (60 mg, 1.7 equiv) was added as a powder to the vial, and then NaOH (0.46 mmol, 1 equiv) was added along with 500 μL of water; the resulting solution was stirred. The pH was adjusted to 10 (pH paper) with 5 μL aliquots of 5 N NaOH, and the solution was stirred. After 3 h, it was applied directly to a 1 mL column of AG 50W-X8 resin, washed with water, eluted with 10% aqueous pyridine, and dried under vacuum attached to a rotary evaporator. The protecting group was removed by stirring with 4 N HCl in ethyl acetate for 0.5 h at room temperature resulting in **11** (33.7 mg, 0.14 mmol, 30%). Specific radioactivity was determined to be 2.5 mCi/mmol, and radiopurity to be 96% by TLC (10% NH<sub>4</sub>-OH/MeOH or 10% HOAc/MeOH). Radiopurity was increased to 99% by loading **11** onto 1 mL of AG50W-X8 resin and washing with water, 10% aqueous pyridine, water, and 1 N HCl. Compound **11** was eluted with 4 N HCl and dried by vacuum rotary evaporation. The product coeluted with authentic L-NIO (**5**) by TLC (10% NH<sub>4</sub>OH/MeOH or 10% HOAc/MeOH).

***N*<sup>α</sup>-Hydroxy-*N*<sup>5</sup>-(1-iminoethyl)-L-ornithine (**12**).** *N*<sup>α</sup>-Boc-L-ornithine (2.82 g; 12.16 mmol) was dissolved in 56 mL of methanol, and then ethyl *N*-hydroxyacetimidate (10 g, 97 mmol) was added all at once. The reaction mixture was adjusted to a basic pH with 2 N NaOH and was allowed to react for 48 h at room temperature. The desired compound was then purified from the reaction mixture by silica gel chromatography (1:2 CHCl<sub>3</sub>/MeOH) followed by a silica gel plug washed with 4:1 CHCl<sub>3</sub>/MeOH and eluted with MeOH. The resulting compound had slight impurities which were removed by silica gel chromatography (1:5 CHCl<sub>3</sub>/MeOH), leaving *N*<sup>α</sup>-Boc-*N*<sup>ω</sup>-hydroxy-*N*<sup>5</sup>-(1-iminoethyl)-L-ornithine (1.18 g; 4.08 mmol; 34%): <sup>1</sup>H NMR (D<sub>2</sub>O)  $\delta$  1.39 (s, 9 H), 1.45–1.85 (m, 4 H), 1.92 (s, 3 H), 3.20 (t, 2 H), 3.86 (m, 1 H); <sup>13</sup>C NMR (D<sub>2</sub>O)  $\delta$  12.96, 26.70, 27.74, 28.57, 41.51, 55.69, 81.01, 133.39, 157.68, 179.87; FAB<sup>+</sup> HRMS, C<sub>12</sub>H<sub>24</sub>N<sub>3</sub>O<sub>5</sub>: M·H<sup>+</sup><sub>obs</sub> = 290.171 45; M·H<sup>+</sup><sub>calcd</sub> = 290.171 60.

The above compound (1 g, 3.5 mmol) was dissolved in 7 mL of 4 N HCl dioxane and stirred at room temperature for 30 min. Volatile

solvents were removed by high-vacuum rotary evaporation to yield **12** (0.8 g, 3.1 mmol, 89%): [α]<sub>D</sub> = +40° (6 N HCl); <sup>1</sup>H NMR (D<sub>2</sub>O)  $\delta$  1.6–2.05 (m, 4 H), 2.17 (s, 3 H), 3.43 (t, 2 H), 4.02 (t, 1 H); <sup>13</sup>C NMR (D<sub>2</sub>O)  $\delta$  12.73, 24.65, 26.96, 42.05, 52.92, 161.37, 172.332; M·H<sup>+</sup><sub>obs</sub> = 190.1184, M·H<sup>+</sup><sub>calcd</sub> = 190.1192. For elemental analysis, an analytical sample of **12** was recrystallized as the monofluinate salt. Calcd for C<sub>17</sub>H<sub>21</sub>N<sub>3</sub>O<sub>11</sub>S: C, 40.55; H, 4.21; N, 13.92. Found: C, 40.78; H, 4.57; N, 13.76.

***N*<sup>δ</sup>-Acetyl-L-ornithine (**14**).** *N*<sup>α</sup>-Boc-*N*<sup>β</sup>-Cbz-L-ornithine, *tert*-butyl ester<sup>15</sup> (245 mg, 0.58 mmol), was dissolved in 10 mL of methanol and stirred with a catalytic amount of 10% Pd on activated carbon under 1 atm H<sub>2</sub>(g) for 15 h. The resulting solution was filtered through Celite. Volatile solvents were removed by rotary evaporation to yield a white powder, which was subsequently dissolved in CH<sub>2</sub>Cl<sub>2</sub> and cooled on ice. First acetyl chloride (50.2 mg, 0.64 mmol) and then triethylamine (70.1 mg, 0.7 mmol in 5 mL of CH<sub>2</sub>Cl<sub>2</sub>) was added dropwise with stirring, and the resulting solution was allowed to warm to room temperature and to stir for 15 h. Volatile solvents were removed by rotary evaporation, and the resulting compound was stirred in 3 mL of trifluoroacetic acid for 1.5 h at room temperature. To this reaction mixture, 30 mL of water was added and the solution was loaded onto 5 mL of AG 50W-X8 resin, washed with water until neutral, and eluted with 1 M NH<sub>4</sub>OH. The ninhydrin positive fractions were pooled and rotary evaporated to a white powder (0.049 g, 0.28 mmol, 48%). Analytical characterization matched literature values for this compound:<sup>56</sup> <sup>1</sup>H NMR (D<sub>2</sub>O)  $\delta$  1.4–1.9 (m, 4 H), 1.93 (s, 3 H), 3.17 (t, 2 H), 3.69 (t, 1 H); <sup>13</sup>C NMR (D<sub>2</sub>O)  $\delta$  21.84, 24.19, 27.77, 38.75, 54.34, 174.19, 174.41; M·H<sup>+</sup><sub>obs</sub> = 175.1064, M·H<sup>+</sup><sub>calcd</sub> = 175.1083.

***N*<sup>5</sup>-(1-Imino-2-hydroxyethyl)-L-ornithine (**13**).** 2-Hydroxyacetimidic acid ethyl ester hydrochloride was synthesized by a procedure similar to literature methods.<sup>57</sup> To a solution of potassium cyanide (13 g, 200 mmol) in 40 mL of water at 0 °C, paraformaldehyde (6 g, 200 mmol) was added in a portionwise manner over 15 min. After an additional 1 h of stirring the mixture was adjusted to pH 2 with 7.5 N H<sub>2</sub>SO<sub>4</sub> and pH 3–5 with Na<sub>2</sub>CO<sub>3</sub> and then extracted with 3 × 15 mL of cold Et<sub>2</sub>O. The organic layers were combined, dried with Na<sub>2</sub>SO<sub>4</sub> and Drierite, and then stirred at 0 °C as dry HCl(g) was bubbled through the mixture for 2 h. The reaction mixture was then concentrated by rotary evaporation until a white product crystallized from solution which, after filtration and drying, gave 2-hydroxyacetimidic acid ethyl ester hydrochloride (7.03 g, 50.4 mmol, 25%): <sup>1</sup>H NMR (DMSO)  $\delta$  1.34 (t, 3 H), 4.33 (s, 2 H), 4.45 (q, 2 H); <sup>13</sup>C NMR (DMSO)  $\delta$  13.60, 58.59, 69.52, 180.13; EI HRMS M<sub>obs</sub> = 103.0620, M<sub>calcd</sub> = 103.0633.

*N*<sup>α</sup>-Boc-L-ornithine (1.1 g, 4.7 mmol) was stirred in 22 mL of water and adjusted to pH 10 with 2.5 N NaOH. 2-Hydroxyacetimidic acid ethyl ester hydrochloride was added portionwise, maintaining pH 9 with concomitant addition of 2.5 N NaOH, until all of the *N*<sup>α</sup>-Boc-L-ornithine was consumed, as shown by TLC. After an additional 45 min of stirring, the pH was adjusted to 7.5, and the reaction was stirred overnight. The reaction mixture was loaded onto 30 mL of AG50W-X8 resin, washed with water, and then eluted with 10% aqueous pyridine. Volatile solvents were removed by high vacuum rotary evaporation to give *N*<sup>α</sup>-Boc-*N*<sup>5</sup>-(1-imino-2-hydroxyethyl)-L-ornithine (*N*<sup>α</sup>-Boc-*C*<sup>ω</sup>-hydroxy-L-NIO) as a pale yellowish oil (0.25 g, 0.87 mmol, 19%): <sup>1</sup>H NMR (D<sub>2</sub>O)  $\delta$  1.65–2.1 (m, 4 H), 3.38 (t, 2 H), 4.12 (t, 1 H), 4.40 (s, 2 H); <sup>13</sup>C NMR (D<sub>2</sub>O)  $\delta$  22.89, 27.00, 41.14, 52.46, 58.09, 166.94, 171.64; M·H<sup>+</sup><sub>obs</sub> = 290.184, M·H<sup>+</sup><sub>calcd</sub> = 290.172.

*N*<sup>α</sup>-Boc-*C*<sup>ω</sup>-hydroxy-L-NIO (0.2 g, 0.7 mmol) was dissolved in 10 mL of 4 N HCl/ethyl acetate and stirred at room temperature for 1 h. Volatile solvents were removed by high-vacuum rotary evaporation to yield a white solid, which was then dissolved in methanol and precipitated as a white solid upon addition of ethyl acetate. Filtration and subsequent drying resulted in the desired compound as a very hygroscopic white solid (0.17 g, 0.6 mmol, 92%): <sup>1</sup>H NMR (D<sub>2</sub>O)  $\delta$  1.36 (s, 9 H), 1.5–1.8 (m, 4 H), 3.29 (t, 2 H), 3.84 (t, 1 H), 4.35 (s, 2 H); <sup>13</sup>C NMR (D<sub>2</sub>O)  $\delta$  22.81, 26.95, 41.04, 52.38, 57.99, 166.91, 171.60; FAB<sup>+</sup> HRMS, C<sub>7</sub>H<sub>16</sub>N<sub>3</sub>O<sub>2</sub>: M·H<sup>+</sup><sub>obs</sub> = 190.119 19, M·H<sup>+</sup><sub>calcd</sub> =

(56) Miller, S. P. F.; Thompson, J. J. *Biol. Chem.* **1987**, *262*, 16109–16115.

(57) McCasland, G. E.; Tarbell, D. S. *J. Am. Chem. Soc.* **1946**, *68*, 2393–2395.

190.119 17. For elemental analysis, an analytical sample of **13** was recrystallized as the monofluorinate salt. Calcd for  $C_{17}H_{21}N_5O_{11}S$ : C, 40.56; H, 4.20; N, 13.91. Found: C, 40.17; H, 4.41; N, 13.45.

***N*<sup>5</sup>-(1-Imino-2-[<sup>2</sup>H<sub>3</sub>]ethyl)-L-ornithine (15, *d*<sub>3</sub>-L-NIO)**. 2-[C<sup>2</sup>H<sub>3</sub>]-Acetimidic acid ethyl ester hydrochloride was synthesized by the method of Burkholder et al.<sup>58</sup> except that ethanol-*d* was substituted for ethanol (56.3 mmol, 55%): <sup>1</sup>H NMR (D<sub>2</sub>O) δ 1.41 (t, 3 H), 4.40 (q, 2 H); <sup>13</sup>C NMR (D<sub>2</sub>O) δ 13.40, 70.12, 179.14. Longer acquisition times also revealed a septuplet at 18.87. For determining HRMS, deuterated samples were dissolved in H<sub>2</sub>O immediately before analysis. FAB<sup>+</sup> HRMS: calcd for C<sub>4</sub>H<sub>6</sub>NOD<sub>3</sub>, M•H<sup>+</sup><sub>calcd</sub> = 90.087 24, M•H<sup>+</sup><sub>found</sub> = 90.086 15.

***N*<sup>5</sup>-(1-Imino-2-[<sup>2</sup>H<sub>3</sub>]ethyl)-L-ornithine (15)** was synthesized by the same route to make L-NIO<sup>41</sup> except that 2-[<sup>2</sup>H<sub>3</sub>]acetimidic acid ethyl ester hydrochloride was used as the starting material and all reactions were carried out in D<sub>2</sub>O (87 mg, 0.34 mmol): <sup>1</sup>H NMR (D<sub>2</sub>O) δ 1.55–2.051 (m, 4 H), 3.23 (t, 2 H), 4.04 (t, 1 H); <sup>13</sup>C NMR (D<sub>2</sub>O) δ 23.00, 27.17, 41.65, 52.51, 164.96, 171.66; FAB<sup>+</sup> HRMS: calcd for C<sub>7</sub>H<sub>13</sub>N<sub>5</sub>O<sub>2</sub>D<sub>3</sub>, M•H<sup>+</sup><sub>calcd</sub> = 177.143 08, M•H<sup>+</sup><sub>found</sub> = 177.141 04.

**Expression and Purification of Recombinant iNOS.** A recombinant murine iNOS/calmodulin overexpression system in *Escherichia coli* was obtained, and the enzyme was purified.<sup>59</sup> The enzyme was quantified according to the methods of Stuehr and Ikeda-Saito<sup>60</sup> using ε<sub>397</sub> = 71 mM<sup>-1</sup> cm<sup>-1</sup> and a MW of 150 kDa.

**Difference Spectra.** Spectra were recorded according to the procedure of McMillan and Masters.<sup>61</sup> Briefly, a solution of 1.55 μM iNOS in 10 μM BH<sub>4</sub>, 10% glycerol, and 100 mM Hepes at pH 7.5 was scanned for absorbance from 370 to 470 nm against a blank containing 10 μM BH<sub>4</sub>, 10% glycerol, and 100 mM Hepes at pH 7.5 in a 100 μL quartz cuvette. Following addition of 1 mM imidazole, another scan was measured over the same absorbance range (subtraction of the first spectrum revealed a type II spectral shift). A 250 μM solution of L-NIO was then added in 2 μL aliquots and scanned over the same absorbance range. The iNOS•imidazole spectrum was then subtracted from each of these to obtain difference spectra. The total volume of aliquots did not exceed 5% of the total volume.

**Initial Velocity Measurements via the Hemoglobin Assay.** The generation of nitric oxide by iNOS was measured by the rapid oxidation of oxyHb to metHb by nitric oxide.<sup>62</sup> The assay mixture contained iNOS (0.1 μM), L-arginine (2 mM), NADPH (0.1 mM), tetrahydrobiopterin (10 μM), dithiothreitol (100 μM), and oxyhemoglobin (7.5 μM), diluted to a total volume of 600 μL with Hepes buffer (100 mM, pH 7.5). The relative rate of nitric oxide synthesis was determined by monitoring the NO-mediated conversion of oxyhemoglobin to methemoglobin at 401 nm on a Perkin-Elmer Lambda 10 UV/vis spectrophotometer. All assays were performed at 30 °C.

**Irreversible Inhibition Kinetics.** iNOS (5–10 μM) was incubated at 37 °C in Hepes buffer (100 mM, pH 7.5), containing catalase (1000 units for kinetic measurements, 100 units for metabolite studies, and none for the experiment in Figure 1), NADPH (9 mM), tetrahydrobiopterin (1 mM), dithiothreitol (10 mM), glycerol (10% v/v), and inactivator in a total volume of 70–550 μL. The reactions were initiated by the addition of iNOS, and 10 μL aliquots were removed to assay for enzyme activity at various times. Controls were performed by omitting the inhibitors or by omitting or replacing NADPH with NADP<sup>+</sup>.

**Irreversibility of Inactivation.** Aliquots (100 μL) of inactivation mixtures were removed at various time points and were subjected to a centrifuged Sephadex G-50 (fine) chromatography column according to the method by Penefsky,<sup>40</sup> except that 100 mM Hepes at pH 7.5 was used as the buffer. Activity was judged using the oxyhemoglobin NO assay as described above.

(58) Burkholder, C. D.; Jones, W. E.; Wasson, J. S. *J. Org. Chem.* **1980**, *45*, 4515.

(59) Rusche, K. M.; Spiering, M. M.; Marletta, M. A. Manuscript submitted for publication.

(60) Stuehr, D. J.; Ikeda-Saito, M. *J. Biol. Chem.* **1992**, *267*, 20547–20550.

(61) McMillan, K.; Masters, B. S. S. *Biochemistry* **1993**, *32*, 9875–9880.

(62) Hevel, J. M.; Marletta, M. A. *Methods Enzymol.* **1994**, *233*, 250.

**Absorbance Spectral Changes during Inactivation.** Spectra were not recorded directly because of high concentrations of NADPH and BH<sub>4</sub> present in the incubation mixtures. Instead, at various time points, 100 μL aliquots of the inactivation mixture were taken and small molecules were removed by centrifuged size exclusion chromatography column according to the procedures of Penefsky,<sup>40</sup> except that the buffers used contained 11% glycerol and 100 mM Hepes. The absorption spectra (350–550 nm) of the collected fractions were recorded in 100 μL cuvettes against a 100 mM Hepes blank.

**HPLC of the Heme Cofactor.** Chromatograms of iNOS (60–250 μg) inactivated by L-NIO (**5**, 45–300 μM) were obtained using gradient elution of an Econosil C<sub>18</sub> HPLC column (Alltech, 10 μm, 250 mm × 4.6 mm) and detection at 400 nm. The elution gradient (1 mL/min) consisted of 5 min of 0% B, 60 min of 5–75% B, and then 2 min of 75–100% B followed by 100% B with buffer A consisting of H<sub>2</sub>O and 0.1% TFA and buffer B of CH<sub>3</sub>CN and 0.1% TFA. The peak at 16 min derived from the BH<sub>4</sub> stock solutions and the peak at 64 min coeluted with heme standards. Chromatograms of iNOS inactivated by [<sup>14</sup>C]-L-NIO (**11**) were obtained using gradient elution (1 mL/min) of an Alltima C<sub>18</sub> HPLC column (Alltech, 5 μm, 250 mm × 4.6 mm) and detection at 400 nm. The elution gradient consisted of 5 min of 0% B and then 80 min of 0–100% B with buffer A consisting of H<sub>2</sub>O and 0.1% TFA and buffer B of CH<sub>3</sub>CN and 0.1% TFA. Fractions (1 mL) were collected, diluted with 15 mL of Ultima Gold liquid scintillation cocktail (Packard), and counted for [<sup>14</sup>C] dpm values.

**Gel Filtration of Inactivated iNOS.** [<sup>14</sup>C]-L-NIO-inactivated iNOS was subjected to gravity flow Sephadex G-50 (fine) column chromatography according to the procedures of Furfine et al.<sup>63</sup> except that 100 mM Hepes was used as the buffer. Fractions of 200 μL were collected, 190 μL of which were counted for [<sup>14</sup>C] dpm and 10 μL of each were used to estimate protein concentration with Coomassie Plus staining reagent (Pierce).

**Dialysis of [<sup>14</sup>C]-L-NIO-Inactivated iNOS.** Samples of iNOS were inactivated with 100 μM [<sup>14</sup>C]-L-NIO as described above (140 μL total volume). After inactivation, these were injected into a Pierce Slide-A-Lyser (10 000 MWCO) and subjected to dialysis against 800 mL of 5 mM Hepes, pH 7.5, at 4 °C. Buffer was changed at 4 or 8 h intervals until no radioactivity was detected in the solvent. The contents of the dialysis chamber was removed, mixed with 15 mL of Packard Ultima Gold LSC cocktail, and analyzed for [<sup>14</sup>C] dpm. Control experiments showed ≥70% protein recovery.

**HPLC of Amino Acid Metabolites.** Inactivation mixtures were derivatized with *o*-fluoraldehyde reagent (Pierce) and injected onto an Econosil C<sub>18</sub> HPLC column (Alltech, 10 μm, 250 mm × 4.6 mm). A Beckman System Gold 125P solvent module was used to control the gradient elution as follows: For samples inactivated with **11**, the gradient consisted of 25–45% B over 10 min followed by 45–75% B over 10 min where the % B was held until all metabolites eluted. For the assay of NOS-mediated conversion of **12** to **14**, the gradient consisted of 35–55% B over 16 min where the % B was held until all metabolites eluted. In each case solvent A consisted of 95% 100 mM NaOAc at pH 7.2, 4.5% methanol, and 0.5% THF. Solvent B consisted of 95% methanol and 5% 100 mM NaOAc at pH 7.2. Sample elution was detected by either absorbance at 340 nm or a Spectra/glo filter fluorimeter fitted with *o*-phthaldehyde fluorescence filters. For counting the radioactivity elution profiles, 0.5 mL fractions were collected, diluted with 5 mL of Packard Ultima Gold liquid scintillation cocktail, and counted for 4 min each in a Packard Tri-Carb 2100TR liquid scintillation analyzer. The [<sup>14</sup>C] dpm values from NIO were counted from the HPLC peak eluting from **12** to 15 min and **12** from 20 to 23 min.

**LC–Electrospray Mass Spectra of Inactivation Mixtures.** Samples of iNOS (864 μg in 140 μL total volume) were incubated with L-NIO (250 μM) for 2.5 h as described earlier either with or without (control) NADPH. Either 25 μL (control) or 30 μL (inactivated) of these samples was injected directly onto a Hypersil XDB C<sub>18</sub> column (2.0 × 250 mm) and using an Applied Biosystems 140 solvent delivery system was eluted at a rate of 190 μL/min with the following gradient:

(63) Furfine, E. S.; Harmon, M. F.; Paith, J. E.; Garvey, E. P. *Biochemistry* **1993**, *32*, 8512–8517.

5–100% B over 80 min, with solvent A consisting of water and solvent B of CH<sub>3</sub>CN. All solvents were 0.5% in formic acid. After 10 min, the column outlet was attached to a Micromass Quattro II mass spectrometer without splitting for monitoring column output using positive mode ionization. Source parameters: capillary voltage 3.43 kV; counter electrode 0.53 kV; cone voltage 84 V; temperature 130 °C; unit resolution scan 550–820 at 2 s/scan. Cone voltage for the MS/MS experiment was 60 V, the collision energy was 40 eV, and the argon gas pressure (the collision gas) was  $3 \times 10^{-3}$  mbar.

**Acknowledgment.** The authors are grateful to the National Institutes of Health for financial support of this work to R.B.S. (Grant R01 GM49725) and to W.F. (NIH Predoctoral Training Grant T32 GM08382). The electrospray mass spectrometer is

supported by an instrument grant from the NIH (S10 RR10485) to R.B.V.B. We thank Professor Michael A. Marletta (University of Michigan) for a generous gift of the cloned *E. coli* cells with an overexpression system for inducible nitric oxide synthase. W.F. carried out all of the experiments except for the HPLC–electrospray mass spectral work with the modified heme. D.N. and R.B.V.B. carried out the HPLC–electrospray mass spectral work with the modified heme.

**Supporting Information Available:** Ten figures of data (12 pages, print/PDF). See any current masthead page for ordering and Web access instructions.

JA982318L